AD-A189 717 CALIBRATION OF A HOT-WIRE/HOT-FILM ANEMOMETER OVER A RANGE OF TEMPERATURE (U) AIR FORCE INST OF TECH WRIGHT-PATTERSON AFB OH D C OKA SEP 87 1/1

UNCLASSIFIED AFIT/GAE/AA/86D-12 F/G 14/2 NL

END

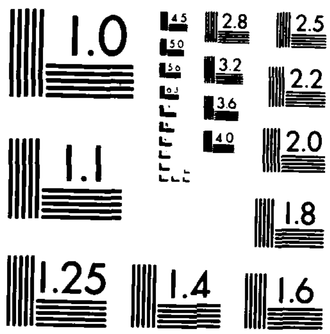

MICROCOPY RESOLUTION TEST CHART
NATIONAL BUREAU OF STANDARDS-1963-A

CALIBRATION OF A HOT-WIRE/HOT-FILM
ANEMOMETER OVER A RANGE OF
TEMPERATURES, VELOCITIES, AND PRESSURES

THESIS

DENISE C. OKA
CAPTAIN, USAF
AFIT/GAE/AA/86D-12

DEPARTMENT OF THE AIR FORCE
AIR UNIVERSITY
AIR FORCE INSTITUTE OF TECHNOLOGY

Wright-Patterson Air Force Base, Ohio

(1)

AFIT/GAE/AA/86D-12

CALIBRATION OF A HOT-WIRE/HOT-FILM
ANEMOMETER OVER A RANGE OF
TEMPERATURES, VELOCITIES, AND PRESSURES

THESIS

DENISE C. OKA
CAPTAIN, USAF
AFIT/GAE/AA/86D-12

AFIT/GAE/AA/86D-12

CALIBRATION OF A HOT-WIRE/HOT-FILM ANEMOMETER OVER A RANGE OF TEMPERATURES, VELOCITIES, AND PRESSURES

THESIS

Presented to the Faculty of the School of Engineering

of the Air Force Institute of Technology

In Partial Fulfillment of the

Requirements for the Degree of

Master of Science in Aeronautical Engineering

Denise C. Oka, BSAe

Captain, USAF

September 1987

Approved for public release; distribution unlimited.

ACKNOWLEDGEMENTS

Recognition is due to the many people without whom I would not have been able to accomplish this task. I would like to extend a very heart felt appreciation and thanks to my advisor, Dr Elrod, for his patience, positive support and long hours; to Dr Richard Rivir of the Aero Propulsion Laboratory for his timely assistance and advice; to Jay Anderson, Leroy Cannon and Nicholas Yardich for all their technical help and patience; to Joe Hofle for fabrication support and to my classmates for their moral support even though they too were very busy. Lastly I would like to give a very special thanks and much love to my husband, Jim, for his love, confidence, and cheerful support during this endeavor.

Denise C. Oka

Table of Contents

<u>List of Figures</u>

List of Tables

Table		Page

List of Symbols

Symbol	Description
A	y-intercept of linear curve fit equation
B	slope of linear curve fit equation
c_p	specific heat at constant pressure ($6057.47 ft^2/sec^2 R$), [ref 9]
C	degrees Centigrade
d	diameter of hot-film, ft.
DSnn...n	DS is shorthand for "Data Set" where nn..n indicates which data set(s) are being evaluated. (e.g. DS123 means that data from calibration runs 1, 2, and 3 are being evaluated)
f	a function of gamma, the ratio of specific heats; f = (gamma - 1)/gamma
F	degrees Farenheit
G	gamma, the ratio of specific heats (G = 1.397), [ref 9]
h	convective heat transfer coefficient
HP	Hewlett-Packard
I	current, amps
IFA	Intelligent Flow Analyzer
k	thermal conductivity
K_{mean}	thermal conductivity at the mean fluid temperature, $volts^2/(ohms\ ft\ R)$
L	Length of hot-film, ft.
Load Factor	Temperature and/or pressure ratio applied to the Nusselt number to compensate for error in choice of reference temperature and/or static pressure. (see eqn.7a, b, c)
M	Mach number
Nu	Nusselt number

Symbol	Description
P	Power, BTU/sec
PI	Platinum-Iridium
PT	pressure transducer
Pr	Prandtl number
P_1, P_2, P_3	different values of static pressure, psia
P_{amb}	standard barometric (ambient) pressure (14.696 psia) [ref 6]
P_o	total pressure, psia
P_s	static pressure, psia
% diff	percent difference between the derived and measured velocities
Q	heat transfer rate, BTU/sec
R	gas constant for air (1716 ft^2/sec^2 R) [ref 9]; used in equation (10)
R	resistance, ohms; used in equation (1)
R	degrees Rankine
Re	Reynolds number
Re_{CF}	Reynolds number derived from linear curve fit equation
R_{ad}	adiabatic cold resistance, ohms
R_{bridge}	IFA-100 bridge resistance (10 ohms)
R_c	sensor resistance at fluid temperature, ohms
R_{cable}	resistance of cable between probe and IFA-100, ohms
R_{hw}	total hardware resistance, ohms
R_{int}	internal probe resistance provided by probe manufacturer, ohms
R_o	sensor resistance when fluid temperature is 0 F, ohms

Symbol	Description
R_{op}	sensor operating resistance for a given operating temperature, ohms
R_{ps}	resistance of probe support, ohms
r_c	recovery factor
rho	density at the mean fluid temperature and static pressure, lbm/ft^3
TSI	Thermo-Systems, Incorporated
T_{aw}, T_{aw}'	adiabatic wall temperature, F or R
T_c, T_f	fluid temperature, F or R; subscript c is usually used in equations involving cold resistance, R_c
T_{mean}	mean fluid temperature, R
T_o	total temperature, R
$T_{o1..o5}$	different values of total temperatures, F
T_{op}	sensor operating temperature, F
T_s	static temperature, R
u, u_{meas}	fluid velocity, ft/sec; calculated from measured pressure and temperature
$u_\perp$	component of velocity normal to the sensor, ft/sec; ($u_\perp$ = 0.707*u)
$u_{derived}$	value of velocity derived from linear curve fit equation (eqn.9)
V	voltage, volts
V_w	voltage across the hot-film, volts
Volts	anemometer bridge voltage, volts
$Volts_1$	anemometer bridge voltage for sensor 1, volts
$Volts_2$	anemometer bridge voltage for sensor 2, volts
X_n	Reynolds number exponent
X_o	Load Factor exponent

Symbol	Description
x	represents Re^{Xn}, the x coordinate input to the linear curve fit routine
x_{der}	represents the value Re^{Xn} derived from eqn.(6) given a value of Nu*Load $Factor^{Xo}$ calculated from measured data
y	represents the value of Nu*Load $Factor^{Xo}$, the y coordinate input to the linear curve fit routine
y_{der}	represents the value Nu*Load $Factor^{Xo}$ derived from eqn.(6) given a value of Re^{Xn} calculated from measured data
αR_c	slope of temperature vs cold resistance curve, ohms/F; α is the temperature coefficient of resistance
μ_{mean}	absolute viscosity at the mean fluid temperature, lbm/ft sec
π	ratio of circle's circumference to its diameter, an irrational constant, $\pi = 3.141593...$

ABSTRACT

An investigation was made of the possibility of developing a single calibration equation that would be applicable to a wide range of temperatures (68 F to 250 F), velocities (150 to 800 ft/sec), and pressures (15 to 33 psia). A platinum hot-film, with a high enough operating temperature to provide good sensitivity to velocity, was calibrated at seven different temperature/pressure conditions. The data was used to calculate velocity, Reynolds number and Nusselt number, and a linear least squares curve fit was applied to the data as a function of Reynolds number raised to an exponent and as a function of Nusselt number times a load factor raised to an exponent. The exponents were chosen, through an iterative process, to provide the best agreement between the data and the curve fit equation. The results indicate that as the range of conditions is allowed to increase so does the error between measured velocity and velocity derived from the calibration equation. The least deviation in velocities occured for curve fits of individual sets of data giving an average of 0.8% to 2.5% difference. When several different temperature or several different pressure curves were curve fit as a single curve the error could be minimized to 2.5% to 3.1% if the velocity range was narrowed to 300 to 700 ft/sec.

CALIBRATION OF A HOT-WIRE/HOT-FILM ANEMOMETER

OVER A RANGE OF

TEMPERATURES, VELOCITIES, AND PRESSURES

I. Introduction

Historically, most hot-wire/hot-film applications and therefore calibrations have been at ambient pressure, in incompressible flow and at relatively low temperatures (ambient to about 150 F). Calibrating under these conditions and over a narrow range of temperatures makes it fairly easy to collapse calibration data to a single curve. However, applications exist, such as in shock tube studies, where it would be desirable to have a single calibration curve that could be applied to a wider range of temperatures, pressures, and velocities and where both incompressible and compressible flow could be accounted for. Little work has been done in this area, with the most notable being McQueen's effort [10]. His work was at ambient pressure for temperatures of 74 F, 175 F and 275 F and velocities from 300 to 900 feet per second. He found that the hot-wire he used (a TSI T1.5 sensor) lacked the sensitivity needed at the higher velocities and temperatures. The best sensitivity achieved was .222 millivolts for each foot per second of velocity. To achieve this the wire had to be operated at or above the maximum recommended operating temperature causing the wire to experience structural and thermal problems.

Objective and Scope

The purpose of this thesis was to look at the feasibility of achieving a single hot-wire/hot-film calibration curve for a wide range of temperatures (68 F to 250 F), velocities (150 to 800 ft/sec), and pressures (15 to 33 psia). Fifteen psia was chosen instead of ambient pressure because this allowed comparison of test data at a common pressure instead of one which changed with the conditions of the day. A hot-film sensor was used so that an operating temperature higher than McQueen's could be achieved. This was expected to enable greater sensitivity and thereby overcome some of the difficulties that he encountered. Fig. 1 shows the specific temperature/pressure combinations that were examined where T_{o1} to T_{o5} and P_1 to P_3 are the total temperatures and static pressures, respectively.

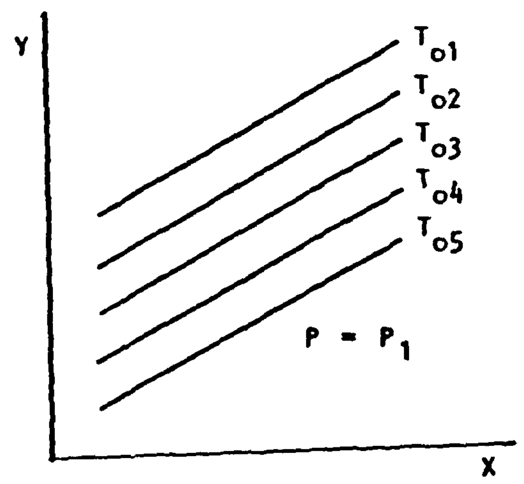

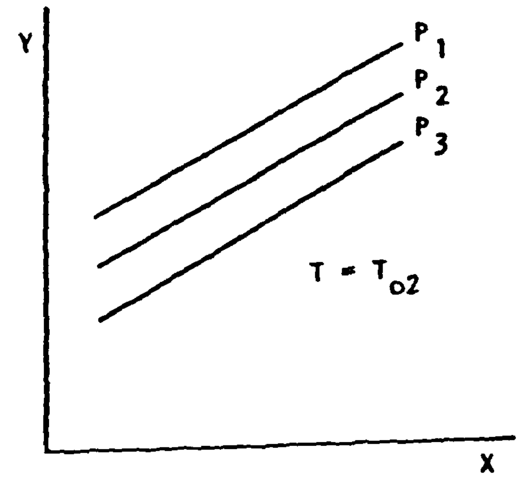

$T_{o1} = 68^oF$	$P_1 = 15$ psia	Vel = 150 to 800 ft/sec
$T_{o2} = 120^oF$	$P_2 = 24$ psia	$X = Re^{Xn}$
$T_{o3} = 160^oF$	$P_3 = 33$ psia	$Y = Nu * \text{Load Factor}^{Xo}$
$T_{o4} = 200^oF$		
$T_{o5} = 250^oF$		

Figure 1: Calibration Conditions

II. Experimental Apparatus

This chapter describes the major pieces of equipment used for this investigation, including the data acquisition system. Some components of the experimental set up were chosen through an evolutionary process and in these cases a synopsis of events is presented.

Calibrator

A schematic of the calibrator used for hot-wire calibration is shown in Fig.2. It was modeled after a TSI Model 1125 calibrator and designed and fabricated by AFWAL's Aero Propulsion Laboratory, Wright-Patterson Air Force Base, Ohio. It was modified by the AFIT Model Shop to enable it to withstand the higher internal pressures of the experiment.

Air was brought in from the inhouse compressors and passed through three filters to remove oil, water, and particulates. At the inlet to the calibrator, the central core of the airflow was dispersed by a very fine mesh screen. The air was heated by four resistance heaters, which were controlled by a Variac autotransformer. The calibrator body was wrapped in fiberglass insulation to help retain heat and reduce temperature gradients along its steel body. The air flow was essentially stagnant until passing through the one-eighth inch diameter nozzle just upstream of the sensor. This particular nozzle diameter was chosen after it had been experimentally determined that a larger nozzle diameter increased the air flow rate beyond the calibrator's ability to heat it for the desired temperature range.

1. air source
2. source pressure transducer
3. inlet valve
4. dispersion screen
5. resistance heater
6. metal screen
7. flow straightening screens
8. bottom thermocouple
9. top thermocouple
10. total pressure transducer
11. static pressure transducer
12. hot-film sensor
13. 1/8" nozzle
14. exhaust valve
15. oil filter
16. dump tube
17. water filter
18. particulate filter
19. very fine mesh screen

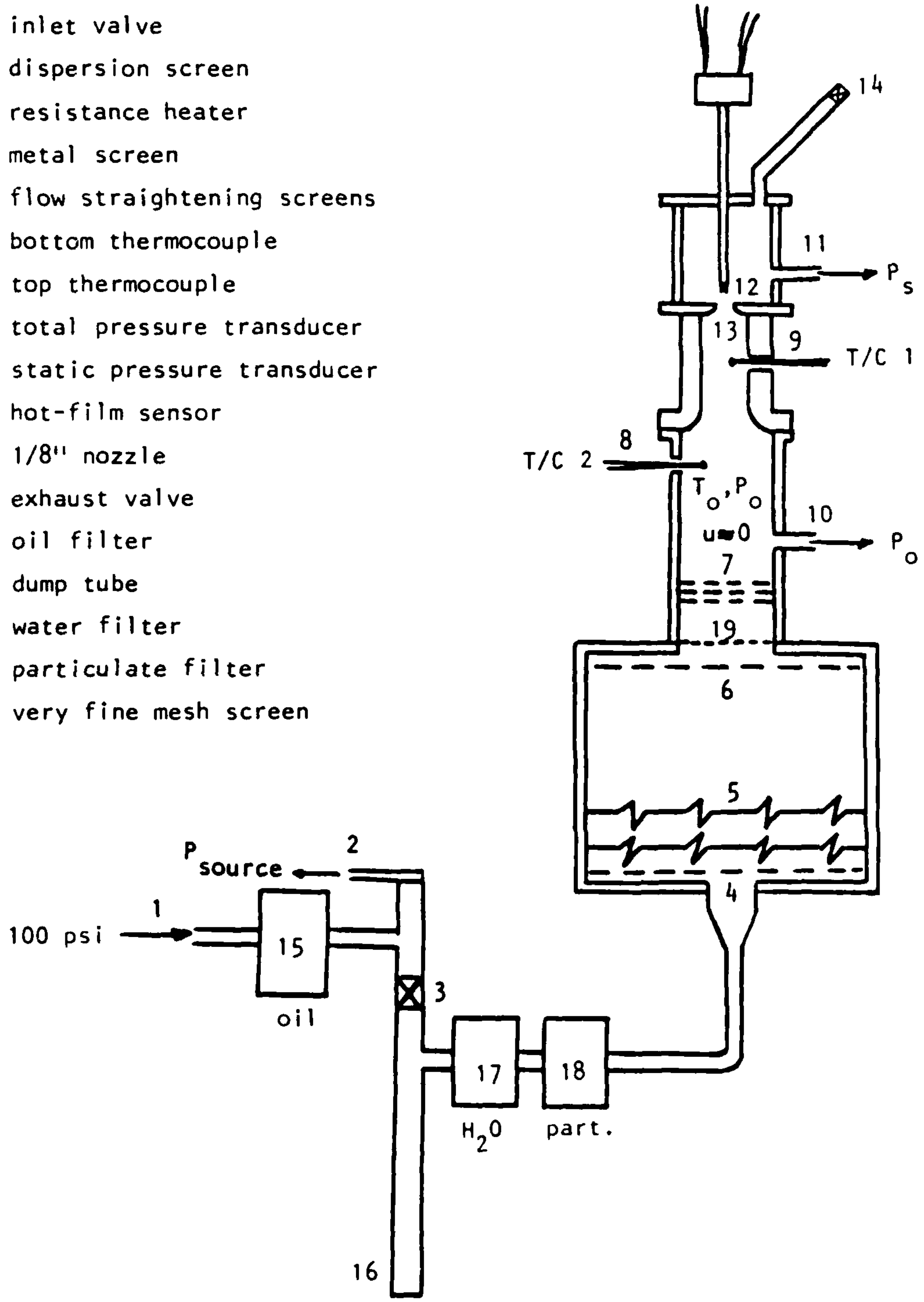

Figure 2: Hot-Wire/Hot-Film Calibrator

Measurement of total temperature and pressure in the chamber upstream of the nozzle was made using two bare wire copper-constantan thermocouples insulated from the calibrator body by ceramic tubing and a 0 to 50 psig pressure transducer, respectively. There was also a second pressure transducer reading taken near the sensor to give static pressure downstream of the nozzle. Air flow rate and static pressure at the sensor were controlled by manipulation of the two valves shown in Fig.2.

Hot-Wire/Hot-Film Anemometer and Sensor

The hot-wire/hot-film measurement system used was a Thermo-Systems, Inc. (TSI) Model 150 Anemometer housed in the TSI IFA-100 Intelligent Flow Analyzer.

The choice of sensor was influenced by the results of McQueen's work [10]. He had used a single tungsten hot-wire with a recommended maximum operating temperature of 300 C (572 F). McQueen operated the wire near this maximum temperature and achieved only marginal sensitivity at higher velocities and temperatures. He also had difficulty not exceeding the structural and thermal limits of the hot-wire.

In order for the sensor to be sensitive to velocity, TSI recommends that the wire temperature be at least 200 C (392 F) greater than the temperature of the fluid in which it is immersed [2]. Because of this and McQueen's observations, the first choice for a sensor was TSI's 1220 PI2.5. This is a high temperature platinum-iridium hot-wire with a maximum operating temperature of 800 C (1472 F) and a diameter of .00025 inches.

Four attempts at calibration were made with the PI2.5, and each time the sensor's wire broke. All breakage occurred with the wires cold, i.e. with no current being applied.

The appearance of the first broken wire indicated that particulate matter had impacted against it (Fig.3). Examination of the probe under magnification revealed small black particles on the wire. It was also noted that part of the broken wire was bent downstream in such a manner as to indicate it had been struck by an object. The calibrator was dismantled, and charred gasket material was seen inside the calibrator assembly. Apparently the calibrator had become too hot for the gasket material causing it to char. It is possible that some of this charred material broke loose and struck the wire. The system was cleaned, the maximum fluid temperature limited to prevent charring and a second PI2.5 wire tried. This too broke, and upon examination under magnification some very fine droplets could be seen on the wire. Inside the calibrator, an oil film was visible in the chamber above the nozzle. The system was again cleaned and filters for oil and particles placed in the air line. The third PI2.5 wire was installed and the heating process started. Before operating temperature was reached, this wire also broke. Water was found in the particle filter and in the elbow and pressure line just below the inlet valve. The inlet valve and elbow were originally located directly below the dispersion screen identified by #4 in Fig.2. It appeared that the pressure and temperature drop caused by the air expanding across the valve was causing water vapor to condense and accumulate. Because of this, the valve location was moved and a dump tube added to allow air expansion to occur prior to the filters (Fig.2, #3 and #16). The particle filter was replaced with a

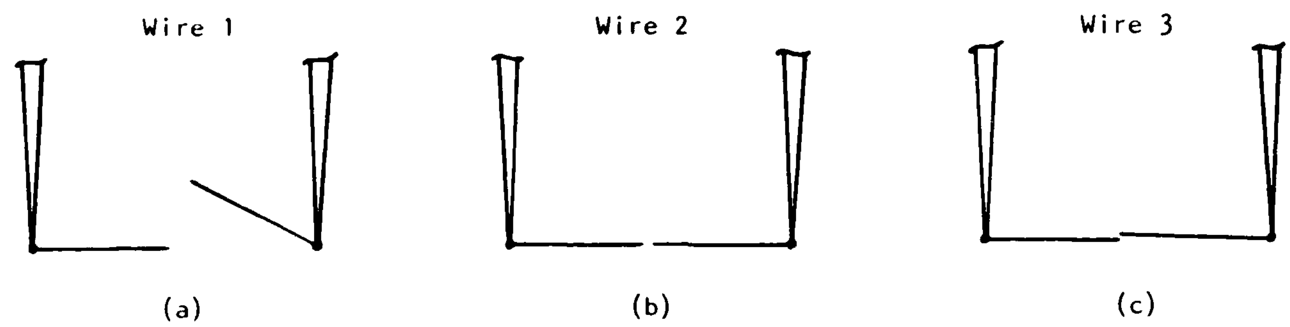

a) Sharp bend in broken wire; particulate viewed under microscope indicates wire was impacted by a relatively large particle.

b) Wire not bent at all but is separated at the center; moisture appears to be on wire, cause of breakage unknown.

c) Very slight vertical separation between the broken ends; no visible cause of breakage.

Figure 3: Appearance of the 1st Three Broken PI2.5 Hot-Wires

dual filter system which removed both water and particles (Fig.2, #17 and #18). A fine wire mesh screen was placed as shown in Fig.2, #19, to prevent very small particles from reaching the wire. These measures taken to clean the supplied air were all that could be done with the time and equipment available. A fourth hot wire was installed, but once again it failed. No cause was visibly identifiable, and, according to the wire's specifications in Reference [13], none of its limits had been exceeded. Except in the case of the first wire, fluid temperature never exceeded about 350 F, ranging between 120 F and 350 F. The maximum allowable fluid temperature for this wire is 1382 F. Velocity was about 300 ft/sec, well below its 1000 ft/sec maximum. Because of the extreme frailty of the PI2.5 hot-wires, other options were reviewed that would still provide the desired higher operating temperature. Platinum hot-films were the next logical choice with a maximum operating temperature of 425 C (797 F). Those available were not designed for high temperature fluids so it was decided to keep fluid temperature less than 250 F to prevent structural problems. This limitation allowed the hot-film to be operated at 645 F providing the temperature difference recommended for good sensitivity and adding a safety margin by staying below the maximum operating temperature. The cylindrically shaped hot-film was chosen over the wedge or cone because its heat transfer equations for data reduction are simpler and well documented.

The particular sensor model chosen was the TSI 1241-10, a dual sensor, end flow, X-film. McQueen had done some work with TSI's 1214-10, a single straight sensor hot-film, and noted that in shock tube applications vibrations occurred. It was hoped that if this sensor were used in a shock tube, the load caused by shock passage would be less due to the sensor's angle to the flow and possibly prevent vibration.

Data Acquisition System

Initially data was taken manually using pressure gages to display gage pressure readings, thermocouples attached to Omega Digicators to give temperature directly in F (or C), and the IFA-100 to read the voltage corresponding to a given velocity and temperature. The source pressure could not be held constant, cycling from a maximum value to some value three to five psi less and then back to a maximum. One instrument reading would be taken each time the source pressure reached its maximum value. This was an extremely time consuming process and provided instrument readings that were not all necessarily at the same source pressure for a given data point.

Automation was the next step. An HP-3052A data acquisition system (Fig.4) became available that was already configured, with software, for hot-wire calibration. With a few minor changes to equipment and modification of the controlling data acquisition program, this system enabled each set of data to be taken automatically and quickly enough to be essentially at the same source pressure. The pressure gages were replaced with pressure transducers and signal conditioners. An existing thermocouple was used for ambient temperature readings. An oscilloscope was used in conjunction with the IFA-100's built-in signal generator to maximize the frequency response of each sensor of the dual sensor hot-film.

All pressure transducer, thermocouple and hot-film sensor signals were brought into the system's voltmeter and processed by the HP-9845

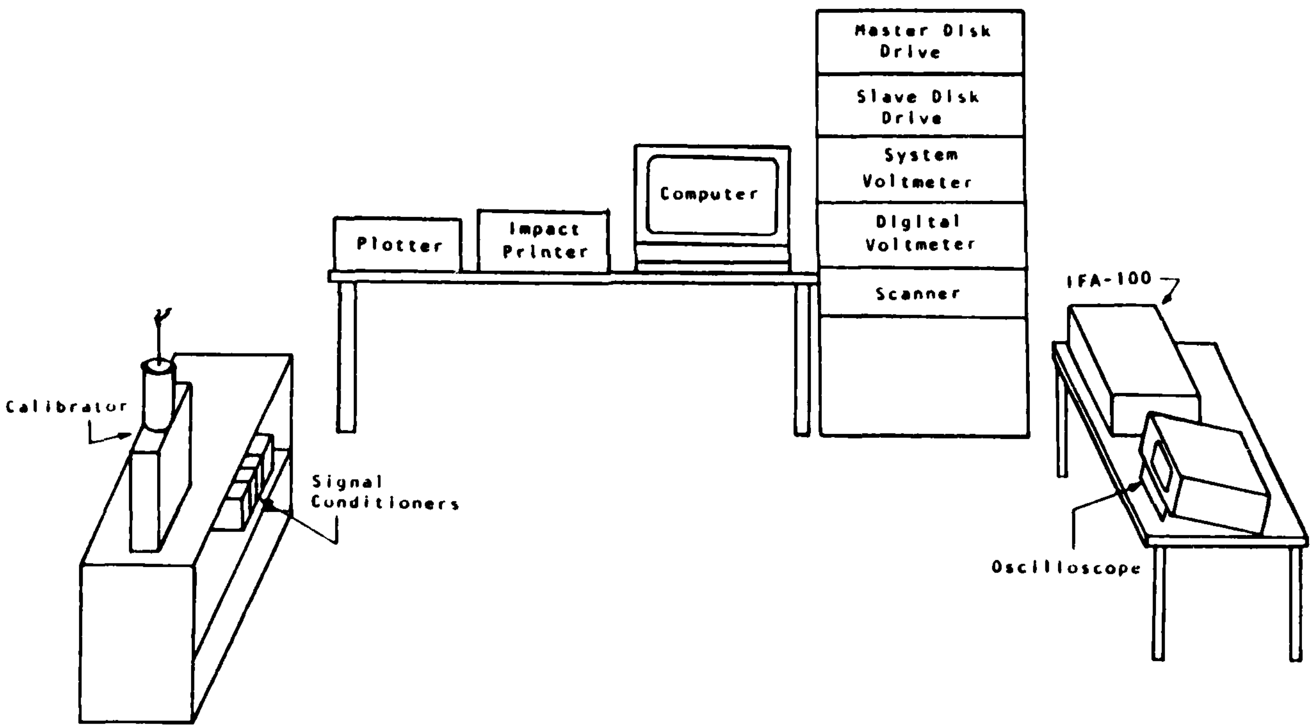

Figure 4: HP-3052A Data Acquisition System

computer. Pressure transducer voltages were converted to gage pressures using predetermined calibration equations. Thermocouple signals were converted to temperatures using an existing HP subroutine. The hot-film sensor voltages were used directly in the heat transfer equations. The data acquisition program enabled the gathered data and some reduced results to be tabulated and plotted.

Pressure Tranducers/Gages

Three gage calibrated pressure transducers were used to measure static pressure by the sensor, total pressure in the calibrator body upstream of the nozzle, and the source pressure. These gage pressures were converted to absolute pressure by adding the standard barometric pressure (P_{amb} = 14.696 psia) [6] to the gage value.

Each transducer was connected to a separate Endevco signal conditioner and all were powered by the same Endevco power supply. Each transducer, its corresponding signal conditioner, and the power supply was calibrated as a single unit using the MKS Portable Vacuum Standard and an HP3438A digital multimeter. The MKS controlled and displayed the pressure being applied to the transducer and the multimeter displayed the transducer's corresponding voltage. The calibrator static and total pressure transducers were calibrated from 0 psig to 41 psig in 5 psi increments. The source pressure transducer was calibrated from 0 to 96 psig in 5-10 psi increments. Straight line equations were calculated for each set of data and were used as the calibration equations in the data reduction program.

The pressure gages that had been part of the manual data acquisition system were left attached to provide a quick look reference for the operator. A list of all equipment used is provided in Appendix C.

III. Theory of Hot-Wire Operation

In the following discussion the term hot-wire will be synonomous with the term hot-film unless otherwise stated.

Hot-wire anemometers are often used to measure fluid velocity and turbulence. The anemometer wire is heated by passing an electric current through it, and then the heat lost by the sensor (wire) to the fluid is measured. The two methods of operating a hot-wire anemometer are the constant current method and the constant temperature method. Of these, the most common (and the one used in this study) is the constant temperature method. This method uses a feedback circuit incorporated into a Wheatstone bridge to maintain the sensor at a constant operating temperature. The amplifier senses changes in voltage due to changes in wire resistance and increases or decreases the current as needed to keep wire resistance and therefore temperature constant.

The anemometer output for the constant temperature system is the voltage output of the amplifier. This voltage is directly proportional to current (V=IR) because resistance is a constant. Note too that the square of this voltage is directly proportional to the heat transfer, Q, from the wire to the fluid since the heat transfer equals the electrical power, P, into the wire [2,4].

$$Q = P = I^2R = V^2/R \tag{1}$$

According to many sources, including Bradshaw [1], heat is transferred out of the wire by radiation, buoyant convection, conduction to the wire's end supports and forced convection due to fluid flow. For the typical wire (and cylindrical hot film), radiation heat loss is only about 0.1% of the input energy and is negligible unless the flow density is very low. Buoyant convection is important only at very low speeds and can be neglected for a typical wire when fluid speeds are greater than 5 cm/sec. For this study both of these sources of heat loss were negligible. Conduction to the supports and forced convection were the main sources of heat loss. Equations relating to the anemometer and heat transfer will be discussed in the section on data reduction.

For more detailed information on the evolution of hot-wire anemometry and its varied uses refer to Reference [5], which provides a comprehensive bibliography of the thermal anemometry work accomplished since 1817.

IV. Experimental Procedure

The first section of this chapter provides an overview of procedures and calculations that had to be accomplished prior to gathering calibration data. The second section describes the data taking process and factors that influenced it.

Pre-Calibration

Prior to calibration the orientation of the sensors' axes to one another was determined to be 90 degrees. The probe was positioned such that flow impinged at 45 degrees to the sensors' axes allowing each sensor to feel the velocity equally (Fig.6). This provided a redundancy factor in that had one sensor broken, the remaining sensor would still have provided enough information to determine flow velocity.

Next the total hardware resistance, eqn.(2), was found and entered into the anemometer's memory [13].

$$R_{hw} = R_{cable} + R_{ps} + R_{int} \tag{2}$$

where:

R_{hw} = total hardware resistance, ohms

$R_{cable} + R_{ps}$ = cable and probe support resistance found using the anemometer and shorting the probe support, ohms

R_{int} = internal resistance of all portions of the probe (Fig.5) except the sensors, ohms; provided by the manufacturer.

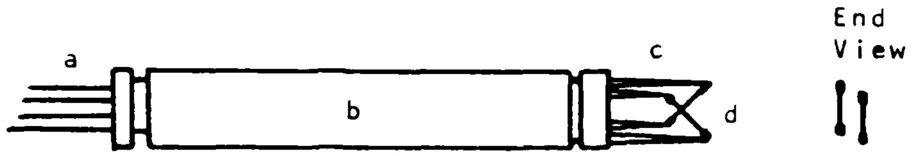

a) pins to insert into probe support

b) probe body

c) sensor supports

d) X-film sensor

Figure 5: Probe Schematic

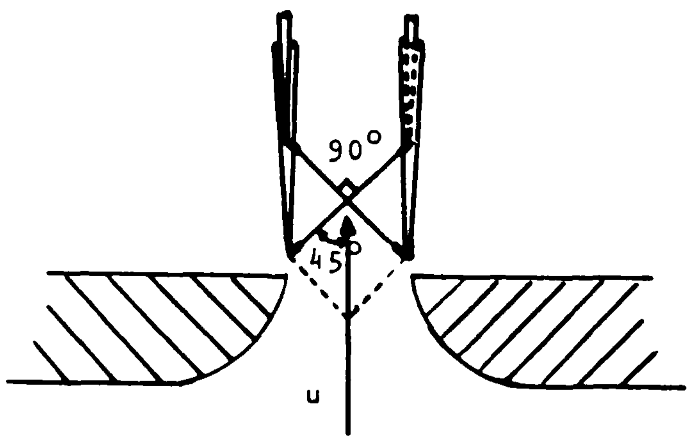

$u_{\perp} = u * \sin 45^{\circ}$

Figure 6: Position of Sensor Relative to the Nozzle and Flow

The anemometer subtracts this value from all subsequent resistance measurements so that actual sensor resistance is measured as a function of fluid temperature. This feature enabled the relationship of cold resistance to fluid temperature to be determined, where cold resistance is defined as the sensor resistance measured when the sensor is 1/16 of an inch downstream of the calibrator nozzle, flow is less than 100 ft/sec and no current is passing through the wire. The flow temperature was varied and a resistance measurement taken at each new temperature. Since no current was heating the wire, the fluid temperature was the sensor temperature. This data resulted in a linear equation [2,13] for each sensor of the form

$$R_c = R_o + (\alpha R_c)T_c \tag{3}$$

where:

T_c = fluid temperature, F

R_c = sensor resistance at T_c, ohms

R_o = sensor resistance when T_c = 0 F, ohms

αR_c = slope, ohms/F

= temperature coefficient of resistance times resistance at temperature T_c

Operating resistance was calculated from eqn.(4) and input into the anemometer which used it to maintain sensor operating temperature [13].

$$R_{op} = R_c + \alpha R_c(T_{op} - T_c) \tag{4}$$

where:

T_{op} = sensor operating temperature, F

R_{op} = sensor operating resistance for a given T_{op}, ohms

T_c = arbitrarily chosen value of fluid temperature, F

R_c = cold resistance for chosen value of T_c, ohms; calculated from eqn.(2)

αR_c = slope corresponding to relevant cold resistance vs. temperature equation, ohms/F

Note that, because of the relationship established between cold resistance and fluid temperature (eqn.3), for a given operating temperature the operating resistance will be a constant regardless of the value of T_c chosen.

Data Acquisition

Calibration was accomplished using the HP-3052A Data Acquisition System and its controlling hot-wire calibration program. The program monitored the voltage signals from the pressure transducers, thermocouples and the anemometer and converted the appropriate signals to psia and F. Velocity at the sensor and pressure and temperature up and downstream of the sensor were displayed for operator use. When the desired conditions were observed, a data point could be taken, recorded and stored. The program automatically stored total temperature (degrees F) and total, static, and ambient pressure values (psia), as well as anemometer voltages for each data point.

Data for seven calibration curves were gathered. Each curve represented a specific temperature/pressure combination over a range of velocities (Fig.1). Ten to thirteen data points were taken for each curve. For each data point, the static pressure was kept within ±0.5 psi of the desired value, the top thermocouple within ±1 F of the calibration temperature and the two thermocouples within ±2 F of each other. This last condition was difficult to achieve at higher velocities and increased temperatures. The difference between the thermocouple readings was as much as 3 to 17 F even after hours of waiting for equilibrium to become established. After discussing this phenomenon with Dr. Rivir [12], it was decided that only the top thermocouple should be used to determine temperature since it was likely that the bottom thermocouple was in either a stagnated or recirculating region.

Calibration of a single temperature/pressure curve generally took 8 to 10 hours where 2 to 3 hours were spent initially bringing the system up to temperature. Any given data point took only seconds to record but achieving the proper conditions could take 10 to 40 minutes of adjusting and waiting for temperatures to equilibrate. Because of calibrator design, the sensor was exposed to the flow for this entire operating time.

V. Data Reduction

The goal of data reduction for this investigation was to generate a linear equation, of the form of eqn.(5), which fit single or multiple sets of data with negligible error. The general calibration equation used to accomplish this was taken from Collis and Williams [3] and Bradshaw [1] and is shown in eqn.(6). The temperature load factor is applied to the Nusselt number to compensate for the effect of using a mean temperature to calculate fluid properties and to aid in the collapsing of data [1,3]. Pressure and pressure/temperature load factors were also investigated for use with data that covered a range of pressures.

$$y = A + Bx \tag{5}$$

$$Nu * \text{Load Factor}^{Xo} = A + B * Re^{Xn} \tag{6}$$

where:

$$Nu * \text{Load Factor}^{Xo} = \text{y-coordinate}$$

$$Re^{Xn} = \text{x-coordinate}$$

$$A = \text{y-intercept}$$

$$B = \text{Slope}$$

$$Xn = \text{Reynolds number exponent}$$

$$Xo = \text{Load factor exponent}$$

$$\text{Load Factor} = (T_{mean}/T_f) \tag{7a}$$

$$\text{or} \quad = (P_s/P_{amb}) \tag{7b}$$

$$\text{or} \quad = (P_s/P_{amb} * T_f/T_{mean}) \tag{7c}$$

T_{mean}/T_f = ratio of mean fluid temperature to measured fluid temperature, R/R

P_s/P_{amb} = ratio of static pressure at sensor to ambient pressure, psia/psia

The constants Xo, Xn, A and B were found through an iterative process. Initially Xo and Xn were chosen to be Xo=-.17 and Xn=.45 or .51 , the values recommended by Collis and Williams [3]. Then a least squares curve fitting routine was applied to the x, y coordinates, Re^{Xn} and $Nu*Load\ Factor^{Xo}$, respectively, to determine A, B and the values of standard error and the percent differences between derived and input values of x and y. Xo and Xn were varied to minimize the standard error and the percent differences. Once the curve fit error was minimized, the resulting values of A, B, Xo, Xn and both the input x and y coordinates and the derived x and y coordinates were tabulated (see Appendix B). Also tabulated were the measured and derived velocities and the percent difference (eqn.8) between the two. The percent difference was used to determine how well the data agreed with the curve fit.

$$\%\ diff = (u_{derived} - u_{meas})/u_{meas} * 100 \tag{8}$$

Measured velocity is given by eqn.(10) and derived velocity is given by

$$u_{derived} = (Re_{CF} * \mu_{mean})/(rho * d * 0.707) \tag{9}$$

where:

Re_{CF} = Reynolds number derived from the curve fit equation, eqn.(6)

$= ((Nu * \text{Load Factor}^{Xo} - A)/B)^{1/Xn}$

These calculations were done for both sensors but only the results relative to sensor 1 are presented in the text since behavior of the two sensors was very similar. Appendix B provides tabulated data for the all graphs displayed in this report and a sample of sensor 2's data for comparison.

To achieve the data reduction described above, the measured temperatures, pressures and voltages had to be converted to more meaningful fluid properties such as velocity, Reynolds number and Nusselt number. Presented below are the equations used to calculate fluid properties and their key variables. Based on data presented in Keenan and Kayes' Gas Tables [9], G, c_p, and R were assumed constant for air over the range of temperatures used in this investigation.

Velocity

It was desirable to know the velocity at the sensor and to use it to calculate Re and Nu. The velocity was assumed equal to the nozzle exit velocity and was derived using eqn.(10) and the measured total temperature and pressure ratio [7]. Because of its positioning (Fig.6), the hot-film senses only the normal component of this velocity.

$$u = ((2/f)RT_o(1-(P_s/P_o)^f))^{0.5} \tag{10}$$

where:

u = velocity, ft/sec

$f = (G - 1)/G$

G = gamma = 1.397

R = gas constant for air = 1716 ft^2/sec^2 R

T_o = total temperature at sensor (top thermocouple), R

P_s/P_o = static to total pressure ratio across the nozzle

Static Temperature

Static temperature was needed to calculate adiabatic wall temperature and therefore Nu. Using total temperature and velocity, static temperature at the sensor is given by [7]

$$T_s = T_o - (u^2/(2c_p)) \tag{11}$$

where:

T_s = static temperature, R

c_p = specific heat at constant pressure

= 6057.47 ft^2/sec^2 R

Recovery Factor

Recovery factor (eqn.12) is a measure of how closely adiabatic wall temperature approaches free stream stagnation temperature [7].

$$r_c = (T_{aw} - T_s)/(T_o - T_s) \tag{12}$$

An approximate value of r_c can be calculated and used to determine adiabatic wall temperature. To determine this approximate value, an adiabatic wall temperature based on adiabatic cold resistance, R_{ad}, (eqn.13) and the T_s and T_o corresponding to R_{ad} are substituted into eqn.(12) [14,12]. Adiabatic cold resistance is defined as the cold resistance of the wire measured at calibration temperature but with flow velocity greater than 100 ft/sec.

$$T_{aw}' = (R_{ad} - R_c)/(\alpha R_c) + T_c \qquad (13)$$

where:

T_{aw}' = adiabatic wall temperature, F

R_{ad} = adiabatic cold resistance, ohms

T_c = arbitrarily chosen value of fluid temperature, F

R_c and αR_c based on eqn.(3) for the chosen T_c

The original data acquisition program required a one time calculation of recovery factor at a desired test velocity and temperature. Test temperature was the calibration temperature, a constant, but velocity could only be an arbitrarily chosen constant, since calibration covered a range of velocities. Because of this, program users chose a velocity somewhere in the middle of the range of velocities and calculated recovery factor there.

For a laminar compressible boundary layer, r_c should be approximately equal to the square root of Prandtl number, about 0.84 for air up to moderately high temperatures [7]. When calculated for this investigation the values were erratic. The equation for recovery factor shows two possible places for error to occur. One is in the calculation of T_{aw}' which is a function of cold resistance and the other is in the measurement of T_o. Total temperature could not be readily doublechecked because of the system design, but the relationship of cold resistance to temperature could. Upon re-examination it was found that the slope of eqn.(3) had increased approximately 3% and the y-intercept had decreased approximately 3%. This change had occurred over a period of about a month. The impact of an incorrect slope on the calculation of T_{aw}' was significant, often causing the adiabatic wall temperature to be less than the static temperature and therefore adversely affecting the calculation of recovery factor. Because of this problem Dr. Rivir [12] recommended the following procedure:

1) calculate recovery factor at room temperature so as to minimize the possibility of temperature being an unknown. The assumption here is that recovery factor does not change significantly with temperature,

2) measure cold resistance "real time"; meaning choose T_c of eqn.(13) to be room temperature and use the anemometer to measure the cold resistance with flow less than 100 ft/sec. Use these values in the calculation of T_{aw}' along with the newly found value of the slope,

3) measure R_{ad} at a series of velocities and calculate T_{aw}' and recovery factor for each,

4) take the average of the recovery factor.

This average value of recovery factor was used in the data reduction program.

Since the cold resistance versus temperature relationship (eqn.3) could effect the values of operating resistance (eqn.4) and therefore Nusselt number (eqn.19), some calculations were made to determine the impact. R_c was calculated using the old and new versions of eqn.(3) and then values of R_{op} and Nu were calculated. The results indicated a negligible impact on all three quantities, showing a 1.1% and 0.9%

difference in R_c, a 0.3% and 0.1% difference in R_{op}, and a 0% and 0.012% change in Nusselt number for sensors 1 and 2, respectively.

Adiabatic Wall Temperature

Eqn.(14) [8] was used to calculate the adiabatic wall temperature of the hot-film with no current applied.

$$T_{aw} = (r_c * u^2)/2c_p + T_s \tag{14}$$

where:

T_{aw} = adiabatic wall temperature, R

u = velocity, ft/sec

Fluid Properties/Mean Fluid Temperature

Since there was a large difference between film and fluid temperatures, the fluid properties, density, thermal conductivity, and absolute viscosity, were calculated as a function of the mean fluid temperature [8] which is given by eqn.(15).

$$T_{mean} = (T_{op} + T_s)/2 + .22(T_{aw} - T_s) \tag{15}$$

where:

T_{mean} = mean fluid temperature, R

T_{op} = operating temperature of the wire, R

Nussselt Number

The Nusselt number is a dimensionless quantity representing heat transfer from the film due to flow over the sensor [4,8]. It is defined as:

$$Nu = hd/k \tag{16}$$

Since Nusselt number is also a function of Re, M and Pr, it is possible through calibration to relate heat transfer, as a function of Nusselt number, to the local velocity at the sensor as a function of Reynolds number. For a constant temperature anemometer, heat transfer equals the square of the voltage across the hot-film divided by hot-film operating resistance [4]:

$$Q = V_w^2/R_{op} = \frac{(Volts * R_{op})^2}{(R_{op} + R_{bridge} + R_{hw})^2} /R_{op} \tag{17}$$

The convective heat transfer is related to Q by [7]:

$$Q = h\pi dL(T_{op} - T_f) = V_w^2/R_{op} \tag{18}$$

Manipulating equations (16, 17, and 18), Nusselt number can be written as:

$$Nu = \frac{Volts^2 * R_{op}}{\pi * L * K_{mean}(R_{op} + R_{bridge} + R_{hw})^2(T_{op} - T_{aw})} \tag{19}$$

where:

$Volts$ = anemometer bridge voltage

R_{op} = operating resistance of the sensor, ohms

R_{hw} = resistance of the hardware, ohms

R_{bridge} = 10 ohms = IFA-100 bridge resistance

L = length of hot-film, ft

K_{mean} = thermal conductivity at the mean fluid temperature, $volts^2/(ohms\ ft\ R)$

Reynolds Number

$$Re = (rho * u_{\perp} * d)/\mu_{mean} \tag{20}$$

where:

rho = density at the mean fluid temperature and static pressure, lbm/ft^3

d = diameter of hot-film, ft

μ_{mean} = absolute viscosity at the mean fluid temperature, lbm/(ft sec)

VI. Results and Discussion

This section presents the results of data reduction for single, multiple, and modified data sets. It also provides a comparison of the results of these groupings.

Individual Data Sets (DS)

Each of the seven data sets was individually curve fit to provide a standard against which to compare the multiple data set curve fits. Figures 7 to 13 represent the best curve fit to each data set where the general calibration equation was

$$Nu(T_{mean}/T_f)^{Xo} = A + B * Re^{Xn} \tag{6}$$

The corresponding exponents, slope and y-intercept for each data set's calibration equation are presented in Table I. Table I also gives the resulting average percent difference in velocity. Velocity percent differences for each data point are provided in Appendix B. The very small deviations shown by the average percent difference indicate good agreement between the data and the derived calibration equation. This is the kind of agreement desired when collapsing data for varied conditions to a single curve. More than one value of average percent difference is shown for DS4, DS6 and DS7. In the case of DS4 the second value represents only the data marked by the circles on Fig.10. Difficulties in achieving the proper calibraton temperature caused the omitted points, marked with triangles, to be recorded 3 to 4 hours later. There is a

TABLE I

Results of Curve Fit for Individual Data Sets

Data Set	Figure	Xn	Xo	y-int, A	slope, B	Avg % Diff in Vel
DS1	7	.51	1.4	1.77	1.38	1.2
DS2	8	.51	1.4	3.01	1.26	.95
DS3	9	.51	1.2	4.07	1.09	.95
DS4	10	.49	1.7	2.10	1.53	1.78[1a]
						.82[2]
DS5	11	.46	1.5	.42	1.7	2.50
DS6	12	.51	1.4	.65	1.68	2.24[1b]
						1.67[3]
DS7	13	.45	1.6	.40	1.65	2.18[1c]
						1.85[4]

(1) includes all data in: a) Fig. 10, b) Fig. 12, c) Fig. 13
(2) accounts for data marked by circles in Fig. 10
(3) does not include lowest velocity data point
(4) does not include highest velocity data point

TABLE II

Results of Curve Fitting DS123 Using Different Load Factors

Load Fac Used	Fig.	Xn	Xo	y-int, A	slope, B	Avg % Diff in Vel
7a	14	.51	1.5	2.65	1.36	3.17
7b	15	.40	0.0	.088	1.47	5.40
7c	16	.41	-.07	.812	1.29	2.84

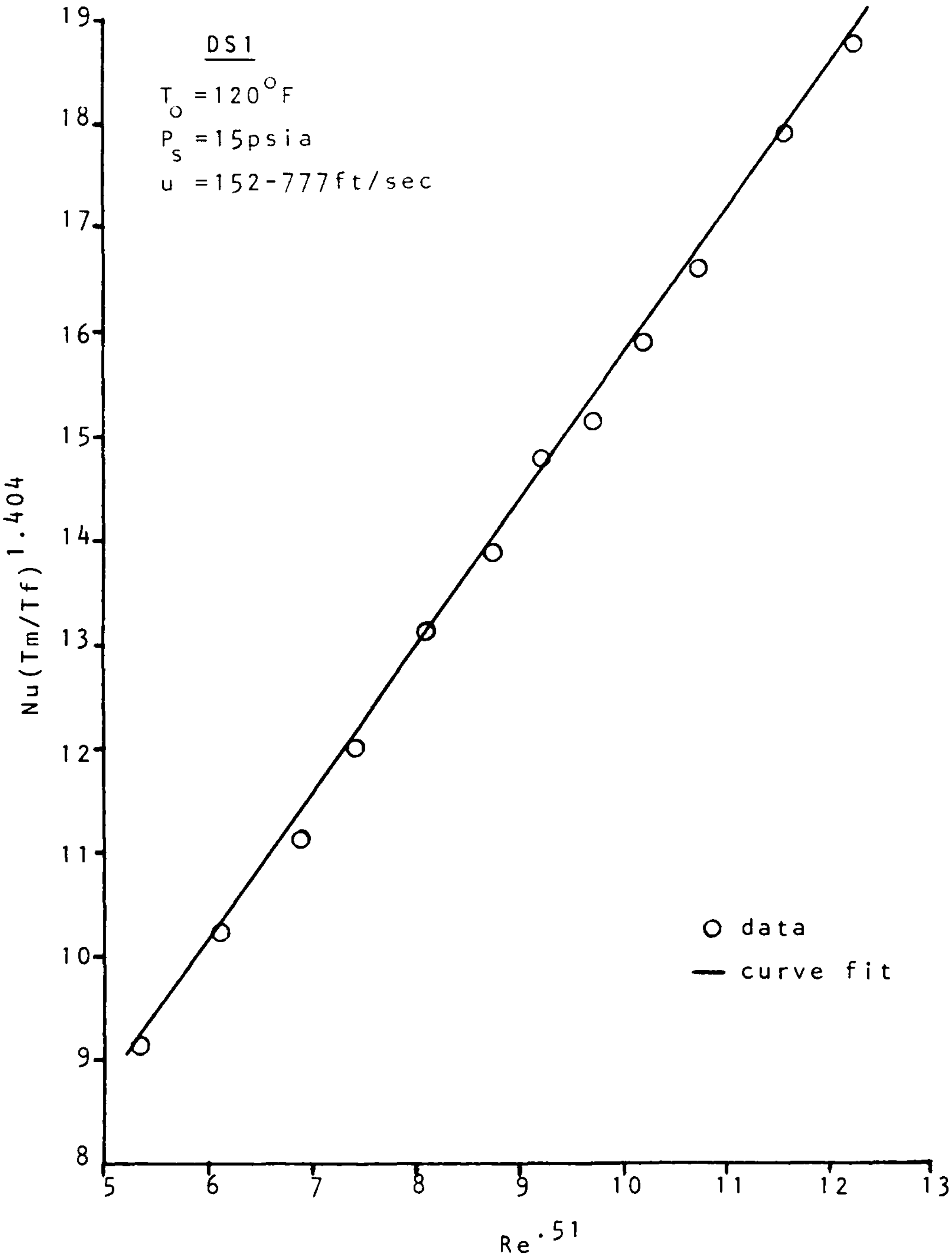

Figure 7: Sensor 1 Data for DS1

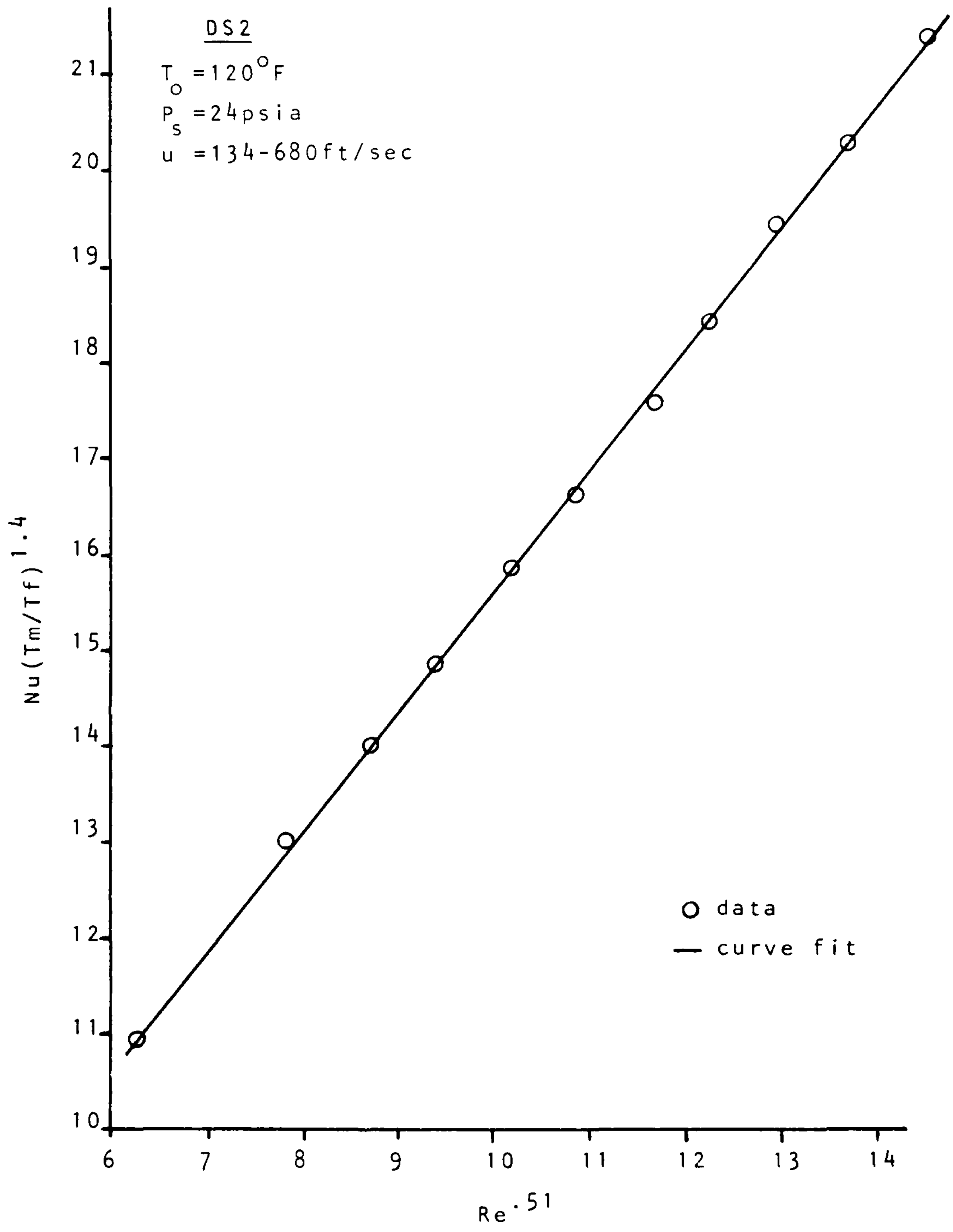

Figure 8: Sensor 1 Data for DS2

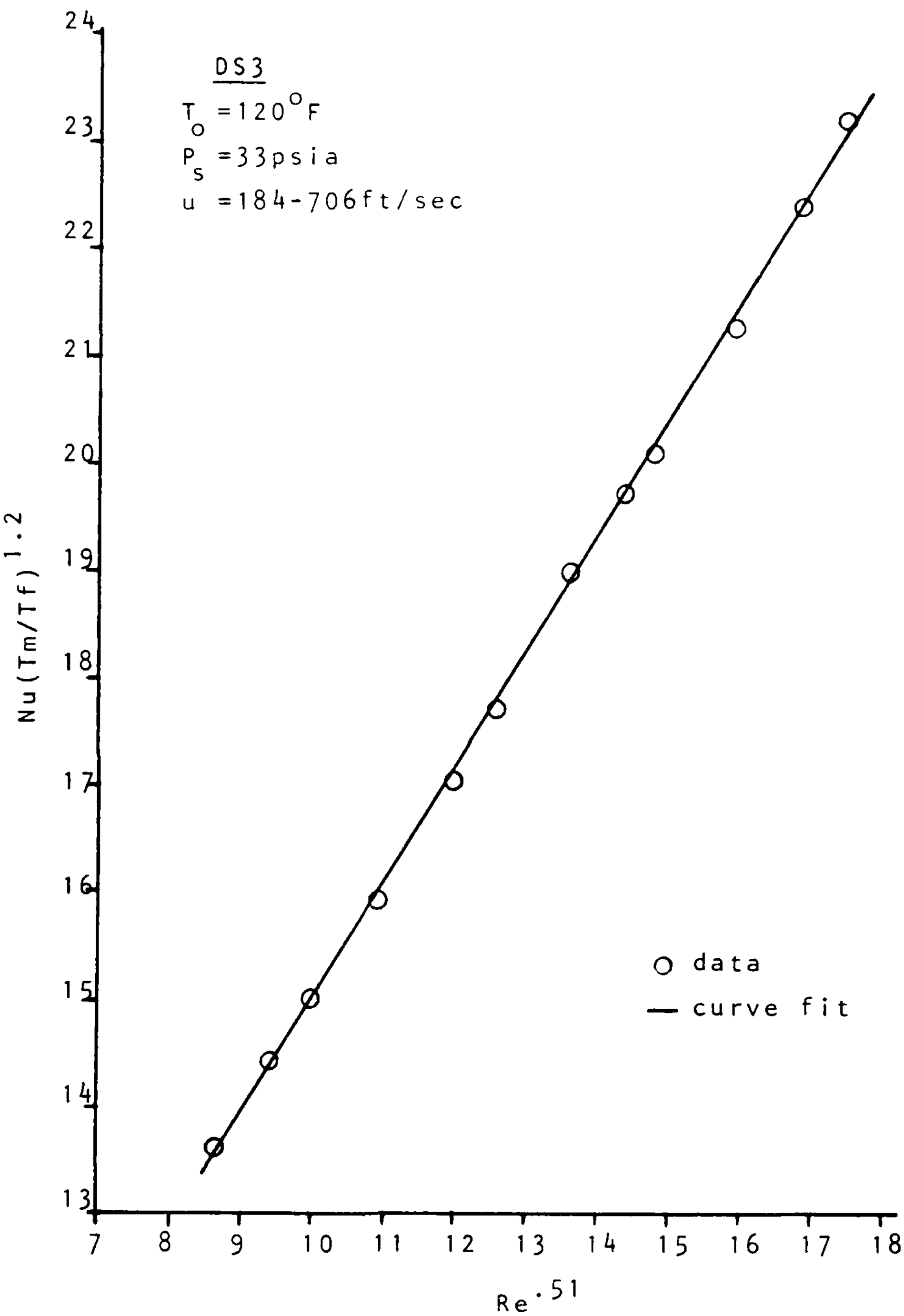

Figure 9: Sensor 1 Data for DS3

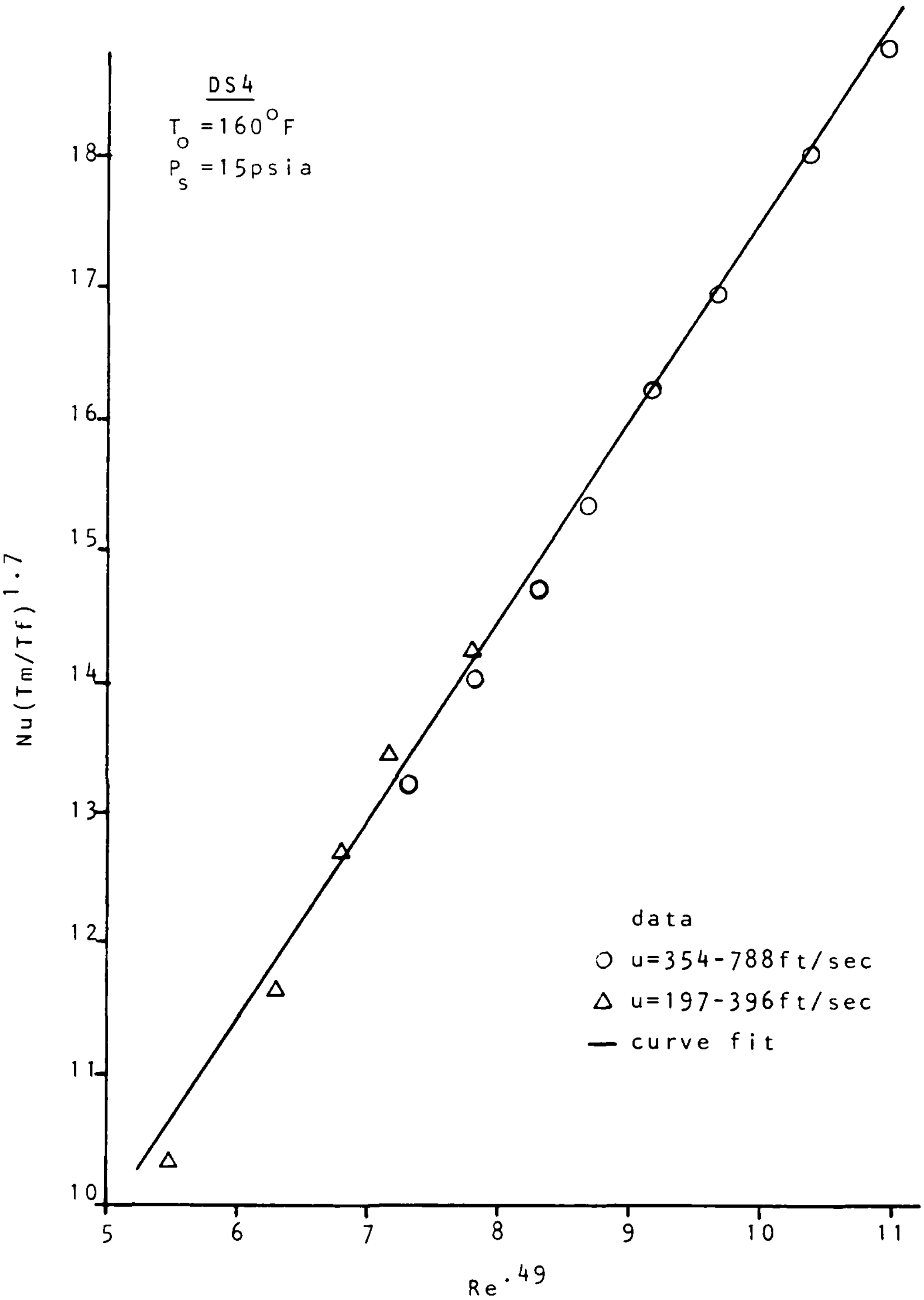

Figure 10: Sensor 1 Data for DS4

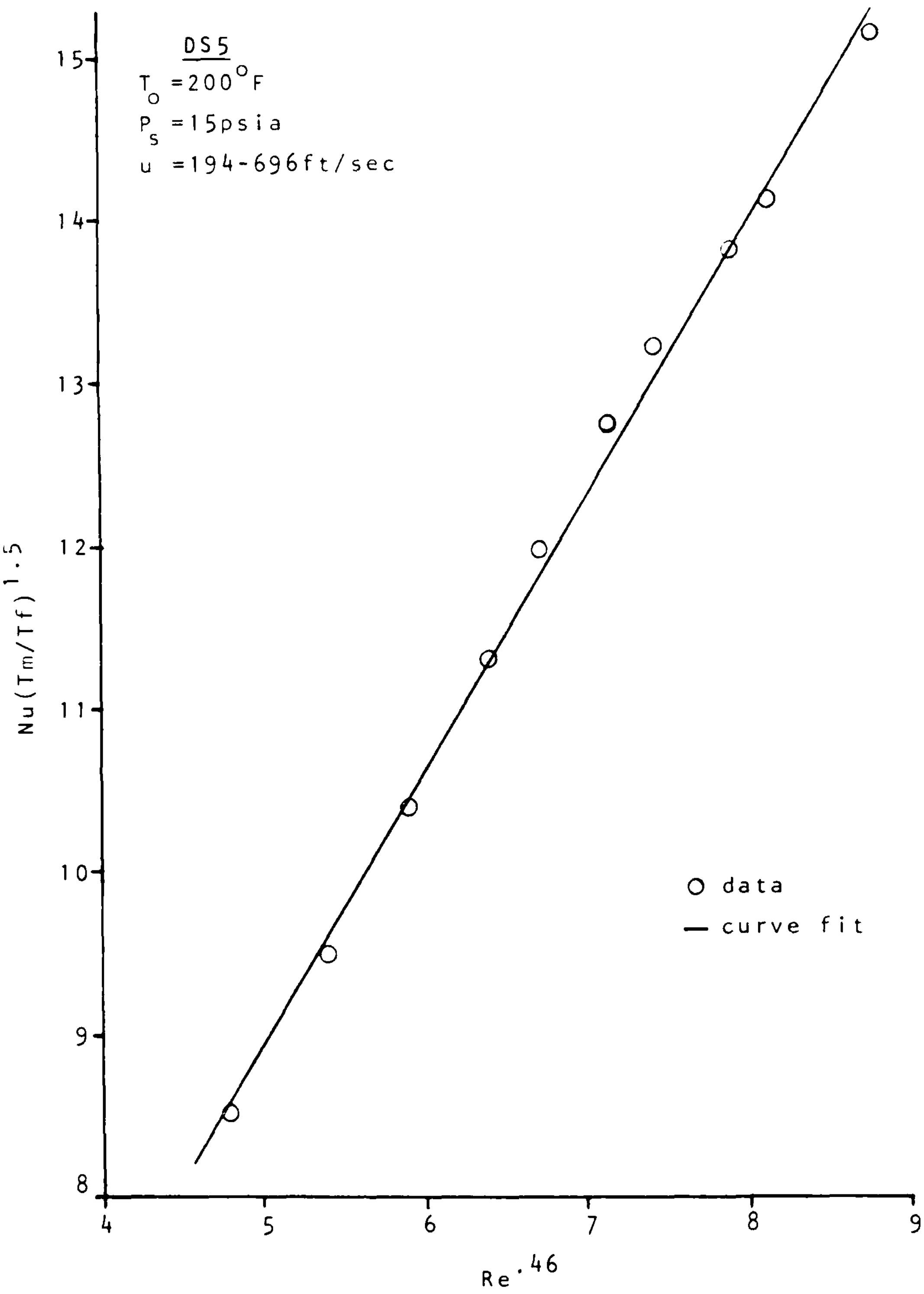

Figure 11: Sensor 1 Data for DS5

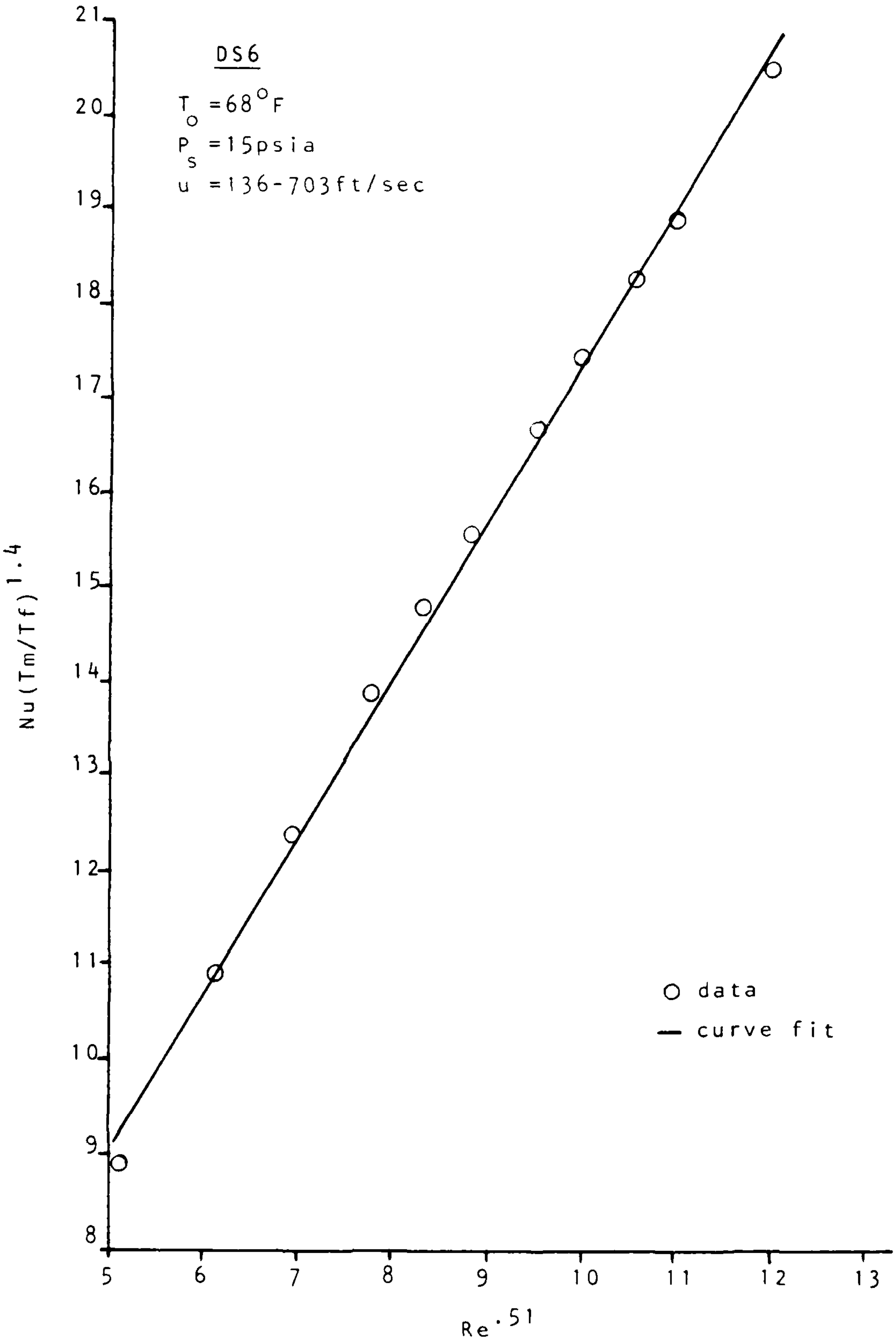

Figure 12: Sensor 1 Data for DS6

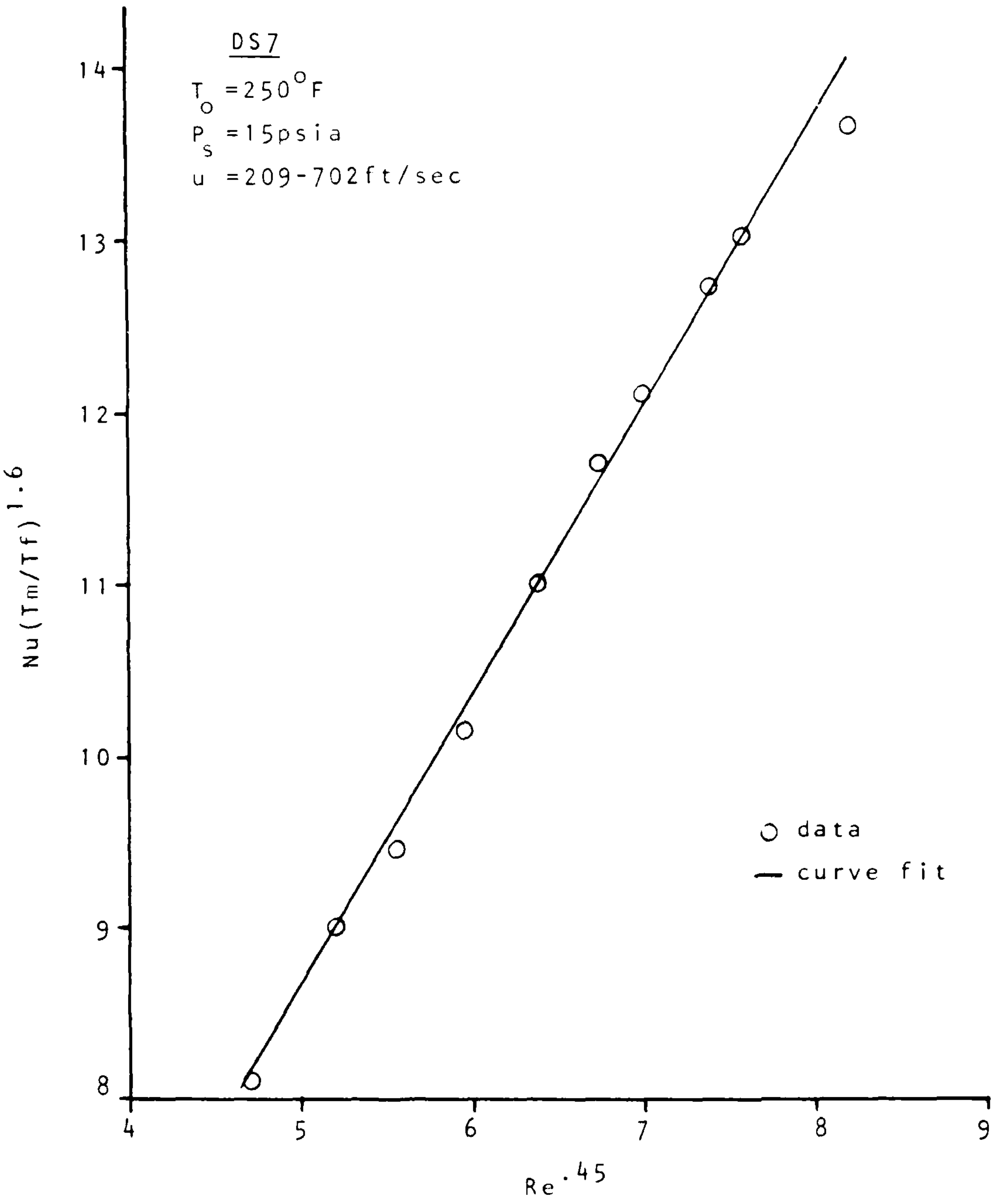

Figure 13: Sensor 1 Data for DS7

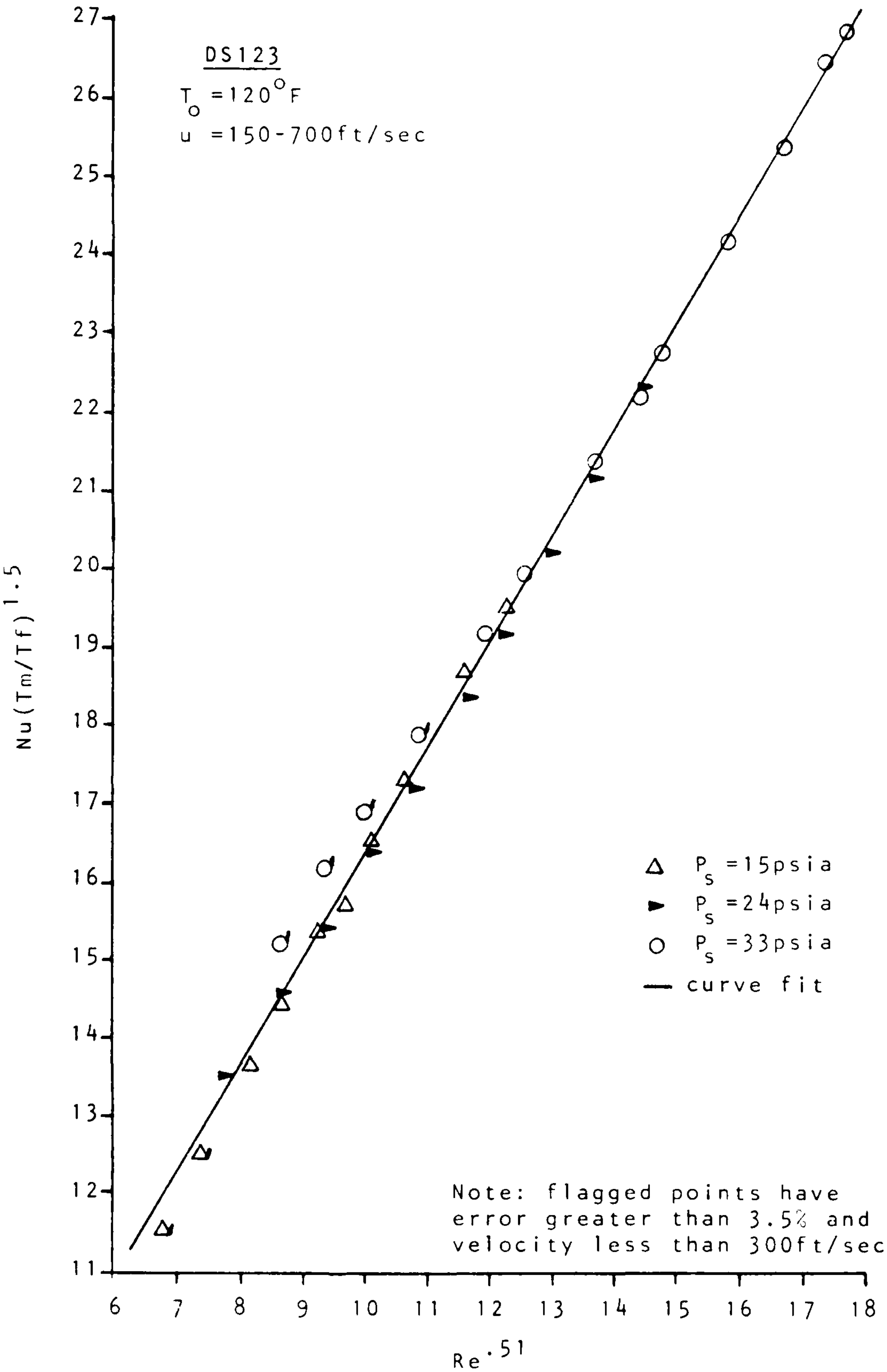

Figure 14: Sensor 1 Data for DS123;
Load Factor = (Tm/Tf) to an Exponent

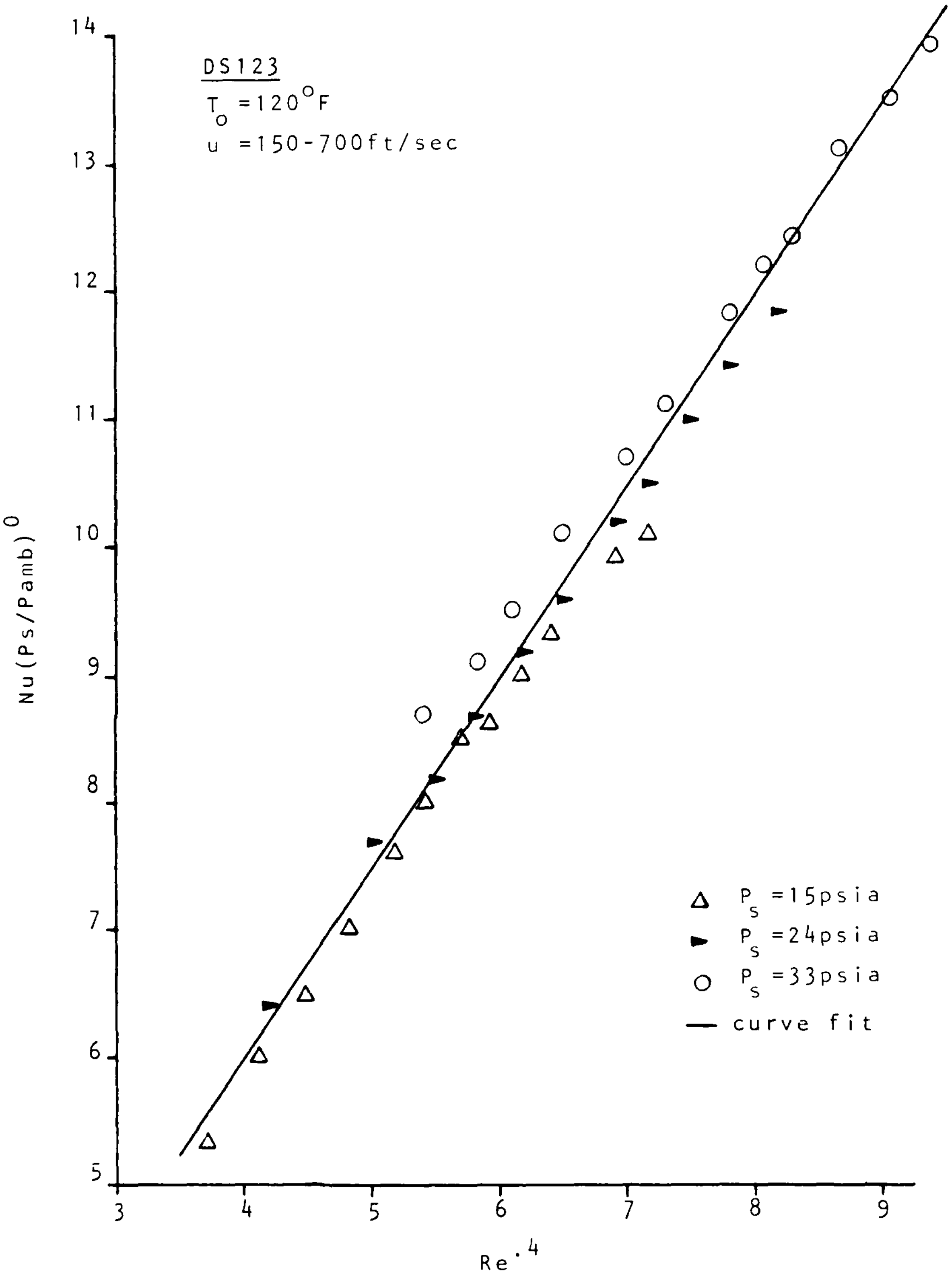

Figure 15: Sensor 1 Data for DS123;
Load Factor = (Ps/Pamb) to an Exponent

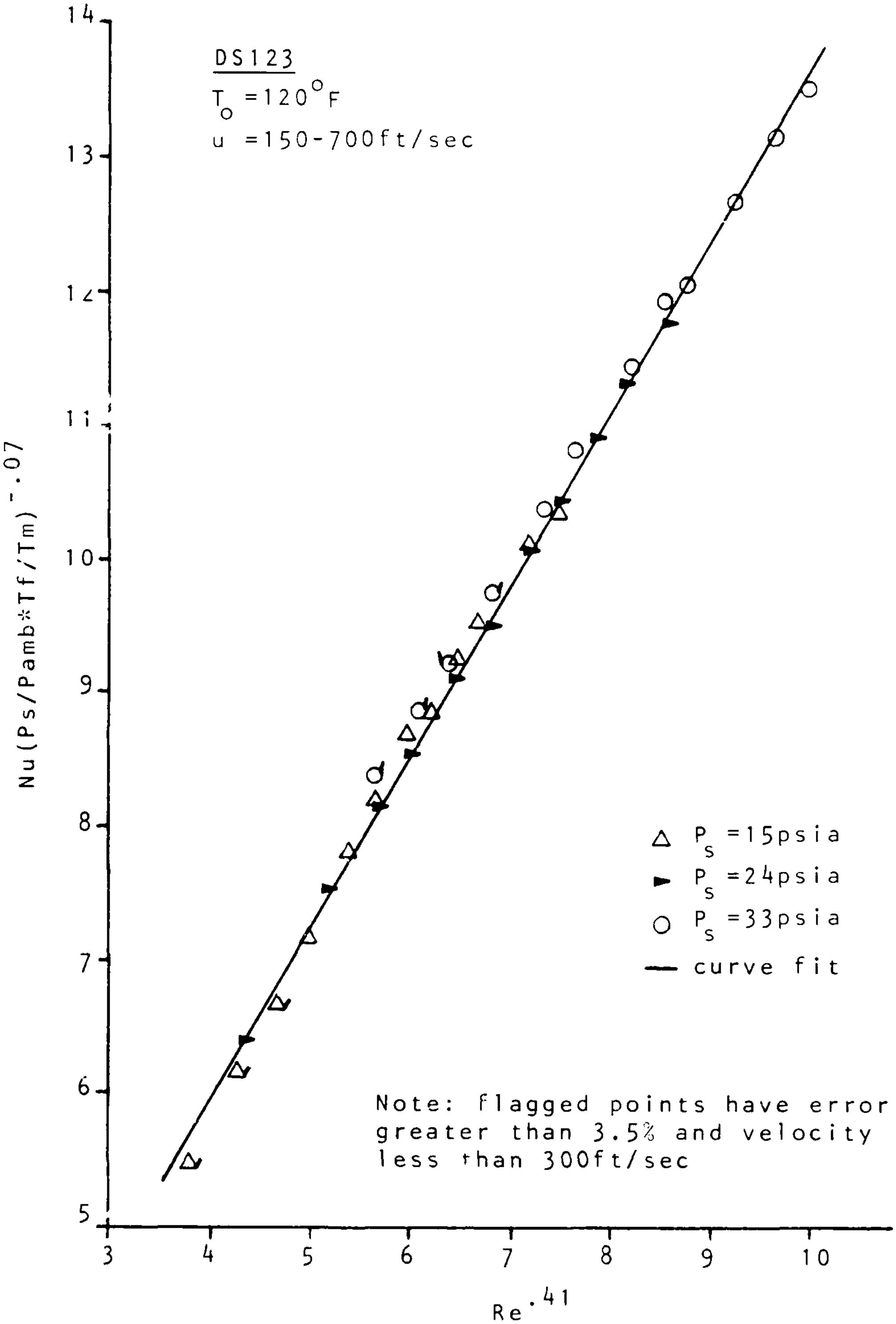

Figure 16: Sensor 1 Data for DS123;
Load Factor = (Ps/Pamb*Tf/Tm) to an Exponent

noticeable change in slope of these later test points which raises the question as to whether this data should be considered separately. For DS6 and DS7 each had one point that was significantly different from the others. For DS6, it was at the low end velocity and for DS7 it was at the high end velocity which implies they may have been poorly taken data points. Results from using the modified data show improved values of the velocity average percent difference.

Combined Data Sets

To attempt the collapse of several data sets to a single curve, the individual data was divided into 2 groups. The first group, DS123, consisted of data from calibration runs 1, 2, and 3 where temperature was 120 F and static pressure varied. The second group, DS14567, contained data from calibration runs 1, 4, 5, 6, and 7 where static pressure was 15 psia and temperature varied.

DS123

Since pressure was a variable for DS123, the effect of a load factor that was a function of pressure was examined as well as the temperature only load factor. The least squares routine was executed using each of the load factors in eqn.(7). From the results presented in Table II and Figs.14 to 16, it appears that the pressure ratio alone is not sufficient to aid in collapsing these three sets of data and the average error for velocity is significant at 5.4%. The temperature only and pressure/temperature load factors provide comparable curve fitting though the average percent difference for the pressure/temperature load factor is slightly better. Both have difficulty with data points whose velocity is less than or equal to 300 ft/sec when pressure is 15 and 33 psia. It appears that the differences in slope for DS1, DS2, and DS3 (Table I) have a noticeable effect on the ability to collapse the data.

DS14567

DS14567 was curve fit using the temperature only load factor (eqn. 7a) since static pressure was constant. Unmodified, DS14567 spanned a temperature range of 68 F to 250 F and velocities from 135 to 788 ft/sec. The results of curve fitting this data are given in Table III and Fig.17. The average percent error in velocity is high, 4.68%, and very few points actually fall on or near the calculated curve. After reviewing the tabulated results (Appendix B), it was obvious that the largest errors, 8 to 27%, occurred where velocity was less than 250 ft/sec or greater than 700 ft/sec. Based on this observation, data points with velocities less than 250 and greater than 700 were removed and a curve fit made of the modified data. The new curve fit showed a significant decrease in the average percent difference (Table IIIb, Fig. 18) dropping it from 4.68% to 2.88% but some of the end points were still 5 to 7% off. In hopes of further reducing the deviation between measured and predicted velocity values, the effect of limiting the temperature range was also examined. This was done in two parts. The first limited the temperature range but retained the full range of velocities. The second limited the temperature and used the narrowed range of velocity from 250 to 700 ft/sec. In each case several temperature ranges were examined. The results, presented in Table IIIc and d, Fig. 19 and 20 and Appendix B, showed that decreasing the spread of the temperature range only, from about 180 F to 80-90 F, had no significant impact on improving the relationship between the data and the curve fit. When done in concert with limiting the velocity there is an improvement where the percent error decreases to 2.5% to 3.13% depending on the temperature range involved. Best results occur for temperatures less than 160 F. Overall it appears that it is the limiting of the velocity range that improves the calibration curve fit when it covers a wide range of temperatures.

Comparing the results shown in Tables I, II and III it can be seen that the best correlation between a linear curve fit and the calibration data occurred when the data set for each temperature and pressure combination was curve fit separately. The collapsed curve fit for DS123 shows promise in that if data taking were restricted to conditions where velocity was greater than 300 ft/sec, the average percent error would decrease from 2.75% and 2.84% to 1.5% and 1.7% respectively. For DS14567, the ability to curve fit over such a wide range of temperatures and velocities is marginal, though it is improved somewhat by the limiting of the velocity range as shown in Table III.

One of the assumptions at the start of this investigation was that if a hot-wire or hot-film with greater sensitivity could be used, then perhaps the calibration data would collapse more readily. The sensitivity for this sensor averaged from 1.7mv/ft/sec at 68 F to 1.1mv/ft/sec at 250 F. This is about five to seven times greater than that achieved by McQueen. During McQueen's calibration he achieved a nominal deviation of 5% between his plotted data and the linear curve fit for a temperature range of 74 F to 275 F and velocities of 389 to 996 ft/sec. In this investigation the nominal percent deviation from the linear was 1 to 2% (Table IV) depending on which set of data was used. DS14567mod is

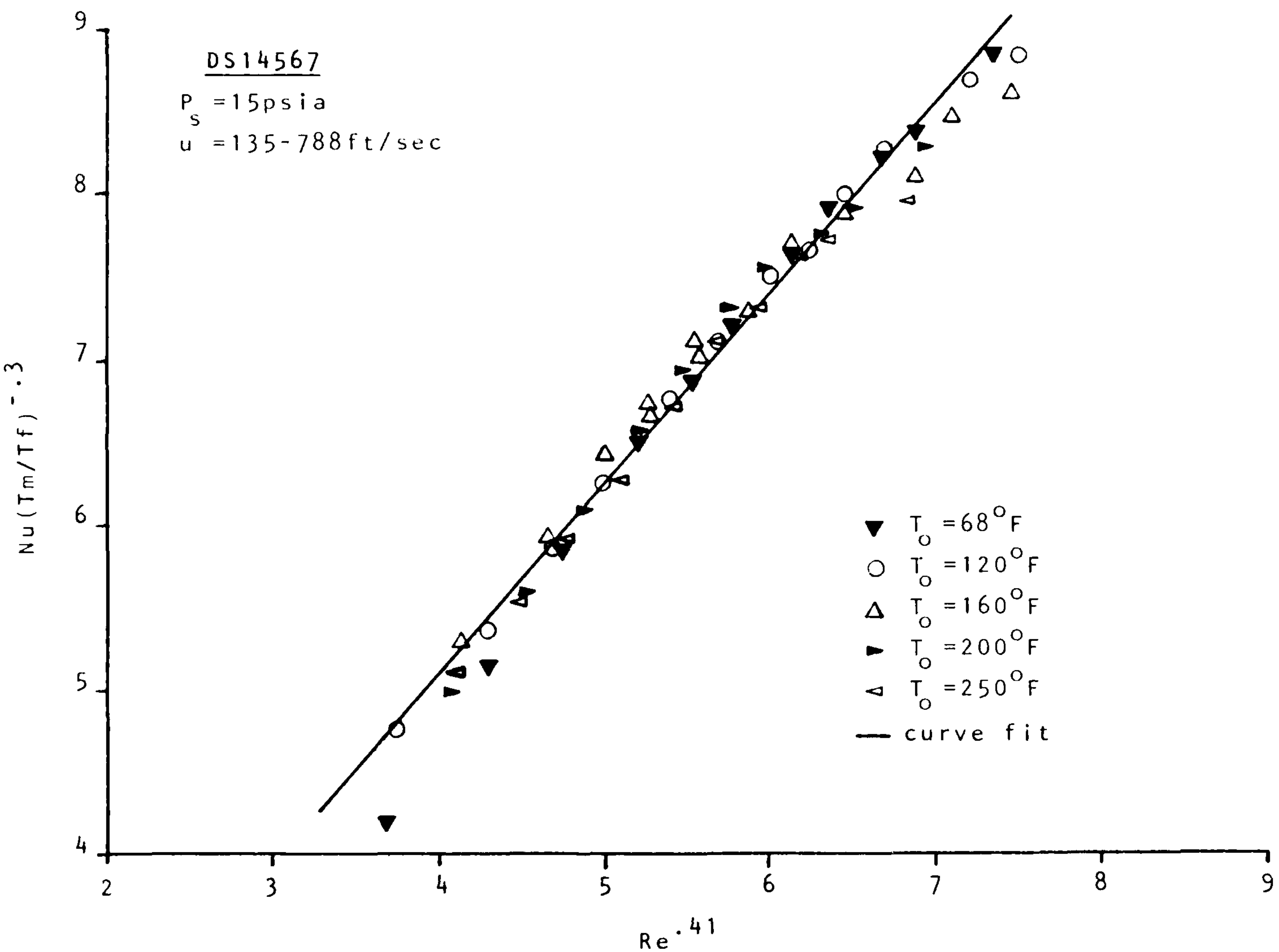

Figure 17: Sensor 1 Data for DS14567;
Full Range of Velocity and Temperature

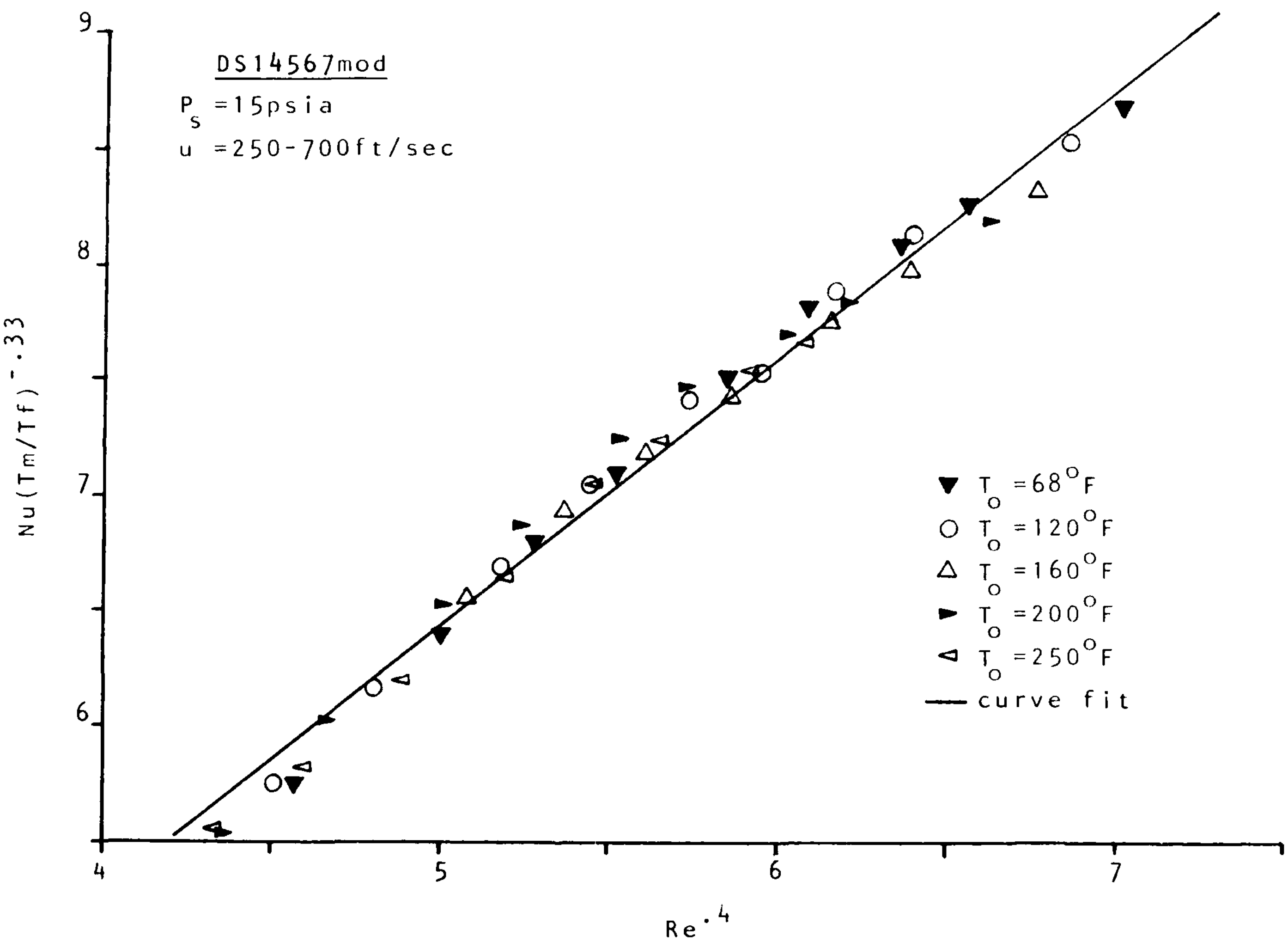

Figure 18: Sensor 1 Data for DS14567mod; Limited Velocity Range

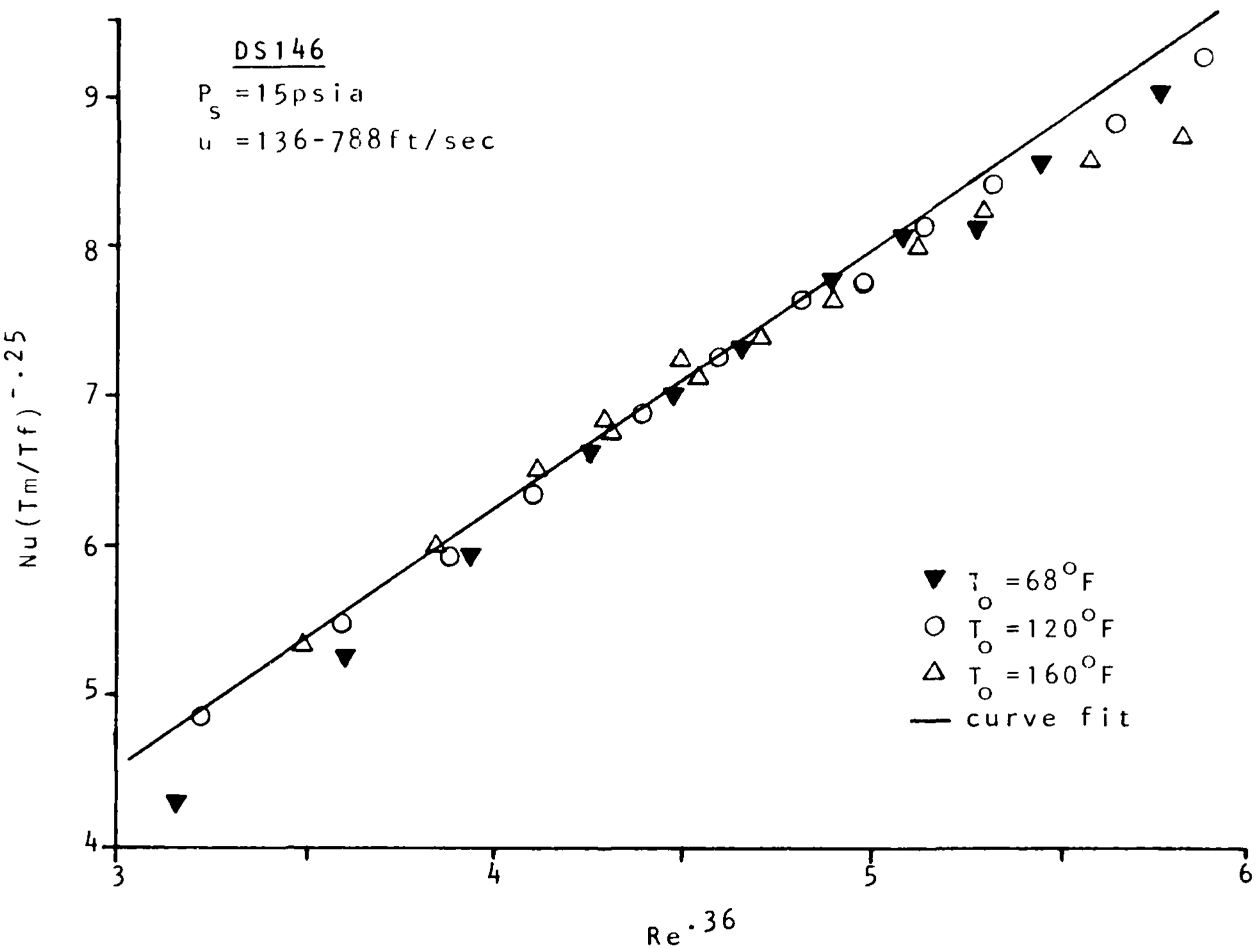

Figure 19: Sensor 1 Data for DS146;
Limited Temperature Range

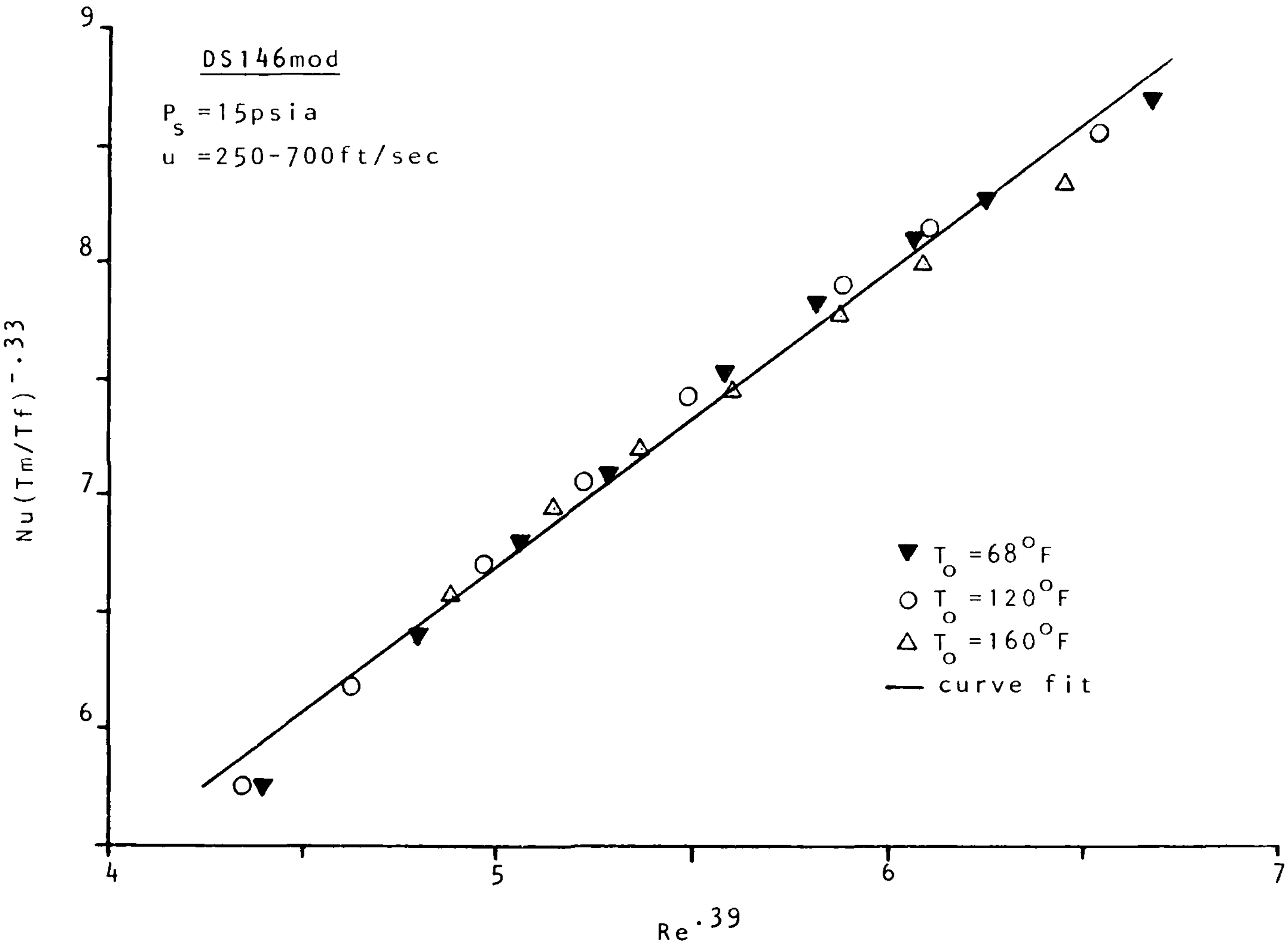

Figure 20: Sensor 1 Data for DS146mod;
Limited Velocity and Temperature Range

TABLE III

Results of Curve Fitting DS14567 and Variations of DS14567

	Data Set/ Conditions	Xn	Xo	y-int, A	slope, B	Avg % Diff in Vel
a)	DS14567* 68-250 F 135-788ft/sec	.41	-.3	.487	1.147	4.68
b)	DS14567mod* 68-250 F 250-700ft/sec	.40	-.33	.460	1.195	2.88
c)	DS146* 68-160 F 135-788ft/sec	.36	-.25	-.417	1.650	4.30
	DS145 120-200 F 135-788ft/sec	.41	-.3	.788	1.100	4.58
d)	DS146mod* 68-160 F 250-700ft/sec	.39	-.33	.389	1.260	2.53
	DS145mod 120-200 F 250-700ft/sec	.4	-.3	.641	1.180	3.13
	DS1457mod 120-250 F 250-700ft/sec	.4	-.33	.263	1.161	3.07

* these data sets are shown in Figs. 17 to 20
** all are tabulated in Appendix B

most comparable to McQueen's data covering temperatures from 68 F to 250 F and velocities from 250 to 706 ft/sec. For this the average deviation was 1.11 to 1.19% depending on whether the x or y coordinate is referred to. This is approximately an 80% reduction in average deviation over McQueen's value.

In McQueen's work, the relative goodness of the calibration equation was based on how low the percent deviation from the linear was. That is, do the values of Re^{Xn} and $Nu*Load\ Factor^{Xo}$ calculated from data taken during calibration match the values derived from the calibration (curve fit) equation?

It is important to note that even if the deviation between data based and derived values of Re^{Xn} and $Nu*Load\ Factor^{Xo}$ is low, it doesn't guarantee that the predicted and actual velocity values will agree as well. This can be seen in Table IV where the average percent difference in velocity is 2 to 3 times greater than the average percent deviation from the linear.

Table IV

Comparison of Deviations from the Linear

Data Set/Conditions	Avg % Deviation from Linear: $x=Re^{Xn}$	Avg % Deviation from Linear: $y=Nu*(\text{Load Factor})^{Xo}$	Avg Pct Vel Diff
DS123 with P/T Load Factor	1.17	1.05	2.84
DS123 with T Load Factor	1.40	1.14	2.75
DS14567	1.94	1.82	4.68
DS14567 with mod	1.19	1.11	2.88
McQueen, 74-275 F, 389-896 ft/sec	5.00 (nominal)		not given

VII. Conclusions and Recommendations

Conclusions

This investigation was designed to determine if calibrating a hot-film with greater sensitivity than a tungsten hot-wire would enable the collapsing of several temperature and pressure curves to a single calibration curve. Based on the results obtained, the following conclusions were made:

1) Greater sensor sensitivity can significantly reduce the average percent deviation of the data from the linear curve fit. However, as can be seen in Table IV, it is evident that the percent difference between measured and predicted velocity must also be accounted for, since it is often two to three times greater than the percent deviation between predicted and measured x-y coordinates of the calibration curve ($x = Re^{Xn}$, $y = Nu * \text{Load Factor}$).

2) Best results will be obtained if a calibration equation is developed for each temperature and pressure condition for a given range of velocities.

3) The more varied the conditions, the more error is introduced. To make use of a single calibration equation for several conditions requires limiting the velocity range (sometimes severely) and accepting a larger degree of error.

Recommendations

Recommendations are given regarding the application of the hot-wire/hot-film anemometer and for improving the facility for this type of investigation.

1) Since sensor sensitivity seems to improve curve fitting ability, experiment with the TSI PI2.5 sensor which has a higher operating temperature and greater sensitivity than either the platinum or tungsten sensors. See if it will enable the collapse of data for a range of different calibration and test conditions.

2) Study the effects of long term exposure of a hot film sensor to conditions where temperature and velocity vary significantly. See if it causes significant changes in the operating characteristics of the sensor such as the relationship between cold resistance and temperature or operating temperature.

3) To reduce time of calibration and of sensor exposure and to improve control of calibration conditions, design a new calibrator system that has easily adjustable and precise temperature (± 1 F), velocity (± 1 ft/sec), and pressure (± 0.1 psi) control; a constant pressure source; variable nozzle sizes to accommodate different sized sensors; an accurate temperature measuring system; and a means of installing the sensor after the calibrator reaches equilibrium.

4) To enable the use of hot-wires that are extremely susceptible to dirty air, develop a reliable means of filtering the air source, possibly by using an electrostatic filter.

Appendix A

Raw Data for the Individual Data Sets

Table V presents the temperature, pressure and voltage data recorded during each calibration run.

TABLE V

Raw Data for Data Sets DS1 to DS7

	$Volts_1$	$Volts_2$	P_s	P_o	T_o
Set #1	2.0452	2.0120	15.040	15.210	120.66
	2.1718	2.1312	14.975	15.297	121.18
	2.2630	2.2160	14.991	15.492	120.85
	2.3484	2.2960	14.978	15.666	119.89
	2.4513	2.3952	15.026	16.027	119.64
	2.5175	2.4636	15.006	16.301	119.45
	2.5920	2.5372	15.002	16.706	119.50
	2.6161	2.5525	14.987	17.045	120.53
	2.6821	2.6205	15.027	17.500	120.53
	2.7291	2.6713	14.986	18.005	121.14
	2.8166	2.7629	14.974	19.386	120.87
	2.8595	2.7984	14.990	20.590	120.36
Set #2	2.2463	2.2017	24.082	24.303	120.76
	2.4515	2.3923	24.076	24.600	120.12
	2.5444	2.4878	23.993	24.801	120.54
	2.6128	2.5576	24.000	25.092	121.02
	2.6925	2.6325	24.067	25.554	120.35
	2.7540	2.6993	24.138	26.038	120.01
	2.8370	2.7897	24.125	26.728	120.42
	2.8908	2.8255	24.088	27.301	120.38
	2.9616	2.8754	24.149	28.206	120.38
	3.0209	2.9326	23.902	28.951	120.97
	3.0860	2.9886	23.975	30.489	120.55
Set #3	2.6039	2.5555	32.974	33.546	121.04
	2.6785	2.6245	33.135	33.926	120.27
	2.7343	2.6845	33.162	34.179	119.70
	2.8129	2.7572	33.086	34.507	120.18
	2.9081	2.8298	33.089	35.136	119.66
	2.9648	2.8798	33.148	35.675	119.62
	3.0584	2.9721	33.160	36.735	120.52
	3.1115	3.0245	32.987	37.399	120.32
	3.1436	3.0528	33.149	38.077	119.97
	3.2289	3.128	33.092	39.579	120.48
	3.2953	3.1947	33.129	41.323	120.64
	3.3511	3.2472	33.005	42.819	120.03
Set #4	2.3416	2.2864	14.997	15.918	159.35
	2.4093	2.3492	15.016	16.229	159.81
	2.4583	2.4012	15.046	16.570	159.70
	2.5047	2.4492	15.001	16.917	160.15
	2.5694	2.5112	15.000	17.470	159.54
	2.6163	2.5544	14.992	18.013	159.60
	2.6832	2.6240	15.017	19.137	160.61
	2.7262	2.6882	15.006	20.364	160.37
	2.0746	2.0439	15.997	15.276	159.84

TABLE V (Cont'd)

	$Volts_1$	$Volts_2$	P_s	P_o	T_o
	2.2013	2.1621	15.003	15.481	160.14
	2.2956	2.2490	14.992	15.689	159.51
	2.3594	2.3089	14.987	15.878	159.51
	2.4272	2.3752	15.004	16.171	159.25
<u>Set #5</u>	1.9382	1.8714	14.989	15.242	200.38
	2.0513	1.9922	14.994	15.418	200.18
	2.1455	2.0851	15.006	15.606	200.17
	2.2394	2.1750	15.000	15.858	200.45
	2.3000	2.2296	15.027	16.104	200.49
	2.3693	2.2943	14.982	16.413	200.26
	2.4105	2.3384	15.029	16.746	200.19
	2.4580	2.3876	14.988	17.234	199.82
	2.4836	2.4134	14.997	17.605	200.82
	2.5587	2.4805	15.000	18.710	199.55
<u>Set #6</u>	2.0053	1.9779	14.993	15.147	68.37
	2.2232	2.1894	15.016	15.337	68.32
	2.3679	2.3274	15.002	15.524	68.29
	2.5016	2.4557	15.006	15.828	68.34
	2.5786	2.5359	15.006	16.089	68.27
	2.6424	2.5994	14.996	16.362	68.29
	2.7265	2.6793	15.014	16.852	68.31
	2.7814	2.7385	14.983	17.267	68.63
	2.8396	2.8045	14.993	17.862	68.56
	2.8763	2.8488	15.011	18.406	68.47
	2.9681	2.9146	14.991	19.908	68.35
<u>Set #7</u>	1.8498	1.7666	15.004	15.278	250.45
	1.9448	1.8618	14.986	15.414	250.68
	1.9962	1.9239	15.005	15.583	250.48
	2.0643	1.9938	15.005	15.788	250.7
	2.1445	2.0722	14.986	16.056	250.56
	2.2136	2.1364	15.001	16.378	250.11
	2.2477	2.162	15.011	16.662	250.87
	2.3039	2.2108	14.991	17.083	250.27
	2.3291	2.2303	14.998	17.409	250.46
	2.3756	2.2595	15.002	18.475	250.97

Appendix B

Calculated Data

This section presents the data that was calculated for each curve fit. The measured and derived velocities (eqns.10 and 9, respectively) and the percent difference (eqn.8) between them are presented for each data point. Also listed are Reynolds number and density (lbm/ft^3). The coordinates used to perform the curve fit are given by x and y where $x=Re^{Xn}$ and $y=Nu*\text{Load Factor}^{Xo}$. These were calculated using the data presented in Table V. The derived values of x and y are also given and can be used to determine the error between plotted values of x and y and the linear curve fit. The derived values were calculated from the curve fit equation (eqn.13) using y to calculate x_{der} and x to calculate y_{der}.

Table VI presents sensor 1 data for the individual curve fits represented by Fig.7 to 13. Samples of data for sensor 2 are given in Table VII, for an individual curve fit, and Tables XVIII to XX for curve fits of multiple sets of data. Note that the exponents providing the best curve fits for sensor 2 are not necessarily the same as those used for sensor 1.

Tables VIII to X give data for the curve fits of data with different pressures, DS123, using the three different load factors. Tables XI to XVII present the data for the curve fits of the different combinations of data, DS14567, at varying temperatures.

TABLE VI

Calculated Data for Individual Curve Fits for Sensor 1

	u_{meas}	u_{derivd}	% diff	Re	rho	x	y	x_{der}	y_{der}
Set #1	152.104	152.337	0.153	25.852	0.048	5.253	9.050	5.257	9.045
	205.643	204.495	-0.558	34.826	0.048	6.115	10.214	6.097	10.239
	255.344	248.543	-2.663	43.372	0.048	6.839	11.112	6.745	11.242
	297.951	296.038	-0.642	50.696	0.048	7.405	11.993	7.381	12.026
	356.476	360.614	1.161	61.024	0.048	8.140	13.110	8.188	13.044
	403.269	409.064	1.437	69.124	0.048	8.674	13.871	8.737	13.784
	458.958	469.126	2.215	78.906	0.049	9.280	14.767	9.384	14.623
	501.628	492.173	-1.885	86.310	0.049	10.163	15.932	10.224	15.846
	544.924	551.418	1.192	94.306	0.049	10.163	15.932	10.224	15.846
	597.093	601.824	0.792	103.415	0.049	10.652	16.584	10.695	16.524
	704.387	705.253	0.123	123.127	0.049	11.643	17.907	11.651	17.897
	777.374	764.746	-1.624	137.138	0.049	12.301	18.667	12.119	18.809
Set #2	134.822	133.788	-0.767	36.672	0.077	6.278	10.890	6.253	10.921
	206.685	212.516	2.821	56.337	0.077	7.815	12.998	7.926	12.857
	256.233	258.182	0.761	69.681	0.077	8.709	14.028	8.743	13.985
	296.868	295.372	-0.504	80.841	0.077	9.395	14.818	9.371	14.849
	344.020	342.406	-0.469	94.202	0.078	10.157	15.779	10.133	15.809
	386.201	382.219	-1.031	106.326	0.078	10.804	16.553	10.747	16.624
	448.419	443.762	-1.038	123.780	0.078	11.675	17.644	11.613	17.722
	494.887	488.551	-1.280	136.81	0.078	12.287	18.391	12.206	18.492
	549.970	550.070	0.018	153.039	0.078	13.009	19.404	13.010	19.403
	609.705	615.405	0.935	168.634	0.078	13.669	20.317	13.736	20.235
	680.228	685.858	0.828	189.996	0.078	14.526	21.392	14.588	21.315
Set #3	184.926	188.434	1.897	68.931	0.106	8.661	13.591	8.745	13.500
	216.346	219.331	1.379	81.169	0.106	9.414	14.391	9.480	14.319
	244.572	245.254	0.279	91.968	0.107	10.034	15.009	10.048	14.993
	288.444	286.685	-0.610	108.339	0.106	10.908	15.908	10.874	15.945
	344.023	341.941	-0.605	129.606	0.107	11.952	17.041	11.915	17.081
	380.224	377.769	-0.646	143.765	0.107	12.601	17.742	12.559	17.788
	448.291	444.553	-0.834	170.069	0.107	13.728	18.951	13.670	19.015
	495.484	488.874	-1.334	187.606	0.107	14.433	19.674	14.334	19.781
	519.998	512.874	-1.370	198.267	0.108	14.846	20.117	14.741	20.230
	589.538	590.446	0.154	225.482	0.108	15.852	21.339	15.865	21.326
	653.219	656.236	0.462	251.459	0.108	16.759	22.355	16.798	22.312
	706.613	719.235	1.786	272.54	0.108	17.461	23.249	17.619	23.077
Set #4	354.361	349.372	-1.408	58.189	0.047	7.628	13.200	7.574	13.278
	404.538	403.089	-0.358	66.644	0.047	8.164	14.024	8.149	14.045
	449.815	445.690	-0.917	74.463	0.048	8.629	14.655	8.589	14.712
	501.415	492.550	-1.768	82.993	0.047	9.110	15.285	9.029	15.401
	563.094	561.453	-0.292	93.667	0.048	9.678	16.195	9.664	16.215
	616.618	617.910	0.210	102.949	0.048	10.146	16.902	10.157	16.886
	706.261	708.186	0.272	118.949	0.048	10.906	17.997	10.921	17.976
	788.933	780.269	-1.098	133.934	0.048	11.573	18.839	11.509	18.931
	197.723	187.739	-5.050	32.265	0.047	5.680	10.278	5.535	10.486

TABLE VI (Cont'd)

	u_{meas}	u_{derivd}	% diff	Re	rho	x	y	x_{der}	y_{der}
	257.739	255.040	-1.047	42.140	0.047	6.492	11.600	6.457	11.649
	309.777	315.691	1.909	50.742	0.047	7.123	12.651	7.191	12.554
	348.912	362.501	3.895	57.233	0.047	7.565	13.397	7.711	13.187
	396.795	417.426	5.199	65.334	0.047	8.083	14.227	8.290	13.929
Set #5	194.506	186.763	-3.981	30.500	0.046	4.817	8.455	4.728	8.606
	250.818	242.048	-3.497	39.415	0.046	5.420	9.482	5.332	9.631
	297.159	296.925	-0.079	46.813	0.046	5.866	10.386	5.864	10.390
	353.618	361.435	2.211	55.804	0.046	6.360	11.338	6.424	11.229
	394.105	407.687	3.446	62.426	0.046	6.697	11.980	6.802	11.801
	452.096	468.561	3.642	71.644	0.046	7.135	12.747	7.253	12.546
	491.215	505.838	2.977	78.282	0.046	7.432	13.222	7.533	13.050
	556.689	555.902	-0.141	88.906	0.046	7.880	13.803	7.875	13.812
	596.104	584.694	-1.914	95.452	0.047	8.141	14.134	8.069	14.257
	696.213	679.641	-3.242	112.602	0.047	8.784	15.125	8.652	15.350
Set #6	135.998	125.280	-7.881	24.297	0.050	5.089	8.843	4.880	9.193
	195.498	193.554	-0.994	35.032	0.050	6.133	10.893	6.102	10.946
	248.365	252.703	1.747	44.539	0.050	6.932	12.390	6.993	12.286
	309.721	318.646	2.882	55.689	0.050	7.769	13.881	7.882	13.691
	353.610	362.613	2.546	63.717	0.050	8.321	14.798	8.428	14.618
	395.026	403.103	2.045	71.289	0.050	8.811	15.594	8.903	15.441
	453.760	461.409	1.686	82.277	0.050	9.480	16.698	9.561	16.562
	502.164	505.395	0.643	91.136	0.050	9.987	17.469	10.020	17.414
	556.507	554.972	-0.276	101.492	0.050	10.551	18.335	10.536	18.360
	599.269	589.156	-1.688	109.82	0.050	10.984	18.927	10.889	19.087
	702.823	687.056	-2.243	129.902	0.051	11.966	20.504	11.828	20.735
Set #7	209.757	206.650	-1.481	31.422	0.045	4.718	8.123	4.686	8.175
	261.510	261.528	0.007	39.180	0.045	5.210	8.988	5.211	8.987
	302.723	294.787	-2.622	45.487	0.045	5.572	9.475	5.506	9.584
	350.912	344.706	-1.769	52.822	0.045	5.960	10.145	5.913	10.244
	408.037	411.775	0.916	61.520	0.045	6.383	10.965	6.410	10.922
	459.691	476.047	3.558	69.605	0.045	6.748	11.699	6.855	11.523
	500.760	511.790	2.203	76.011	0.045	7.021	12.087	7.090	11.973
	559.019	574.299	2.733	85.124	0.045	7.388	12.726	7.478	12.578
	596.469	604.543	1.354	91.104	0.045	7.617	13.032	7.663	12.956
	702.287	666.140	-5.147	108.195	0.045	8.230	13.647	8.036	13.966

TABLE VII

Sensor 2 Data for DS2; $X_n = .45$, $X_0 = 1.4$

	u_{meas}	u_{derivd}	% diff	Re	rho	x	y	x_{der}	y_{der}
Set #2	134.822	133.833	-0.733	36.673	0.077	5.058	10.473	5.3041	10.502
	206.685	207.626	-0.455	56.337	0.077	6.136	12.390	6.148	12.369
	256.233	255.647	-0.229	69.683	0.077	6.752	13.423	6.745	13.435
	296.868	295.196	-0.563	80.843	0.077	7.218	14.212	7.200	14.244
	344.020	341.853	-0.630	94.205	0.078	7.733	15.097	7.711	15.135
	386.201	388.055	0.480	106.330	0.078	8.166	15.915	8.183	15.885
	448.419	460.852	2.773	123.787	0.078	8.744	17.073	8.852	16.886
	494.887	494.760	-0.026	136.827	0.078	9.147	17.582	9.146	17.584
	549.970	542.634	-1.334	153.053	0.078	9.620	18.303	9.562	18.403
	609.705	610.434	0.120	168.654	0.078	10.050	19.157	10.055	19.147
	680.228	677.283	-0.433	190.024	0.078	10.604	20.071	10.583	20.107

TABLE VIII

Calculated Data for DS123; Load Factor = (T_m/T_f)

u_{meas}	u_{derivd}	% diff	Re	rho	x	y	x_{der}	y_{der}
152.104	135.230	-11.094	25.852	0.048	5.253	9.382	4.947	9.798
205.643	187.565	-8.791	34.826	0.048	6.115	10.590	5.834	10.972
255.344	232.534	-8.933	43.371	0.048	6.839	11.524	6.520	11.958
297.951	281.500	-5.521	50.695	0.048	7.405	12.441	7.194	12.729
356.476	348.761	-2.164	61.022	0.048	8.140	13.606	8.049	13.729
403.269	399.593	-0.912	69.122	0.048	8.674	14.401	8.633	14.456
458.958	463.061	0.894	78.903	0.049	9.279	15.339	9.322	15.281
501.628	487.642	-2.788	86.306	0.049	9.714	15.683	9.575	15.872
544.924	550.864	1.090	94.300	0.049	10.163	16.560	10.219	16.484
597.093	604.985	1.322	103.407	0.049	10.652	17.247	10.723	17.150
704.387	717.693	1.889	123.114	0.049	11.643	18.651	11.754	18.499
777.374	783.827	0.830	137.120	0.049	12.300	19.465	12.352	19.395
134.822	138.286	2.570	36.672	0.077	6.278	11.306	6.360	11.194
206.685	214.829	3.940	56.336	0.077	7.815	13.498	7.970	13.287
256.233	258.995	1.078	69.681	0.077	8.709	14.570	8.757	14.505
296.868	294.858	-0.677	80.839	0.077	9.395	15.394	9.362	15.438
344.020	340.216	-1.106	94.199	0.078	10.157	16.398	10.100	16.476
386.201	378.595	-1.969	106.322	0.078	10.804	17.208	10.695	17.357
448.419	437.916	-2.342	123.774	0.078	11.675	18.351	11.534	18.542
494.887	481.201	-2.766	136.810	0.078	12.286	19.138	12.112	19.375
549.970	540.597	-1.704	153.029	0.078	13.009	20.204	12.895	20.359
609.705	603.969	-0.941	168.621	0.078	13.669	21.168	13.603	21.258
680.228	672.612	-1.120	189.977	0.078	14.526	22.311	14.443	22.425
184.926	209.446	13.259	68.930	0.106	8.661	15.213	9.229	14.440
216.346	238.537	10.257	81.168	0.106	9.414	16.119	9.895	15.465
244.572	262.911	7.498	91.967	0.107	10.033	16.821	10.410	16.308
288.444	301.544	4.542	108.337	0.106	10.908	17.839	11.158	17.498
344.023	352.931	2.589	129.603	0.107	11.952	19.133	12.109	18.920
380.224	386.064	1.536	143.761	0.107	12.601	19.937	12.699	19.804
448.291	447.729	-0.125	170.062	0.107	13.728	21.326	13.719	21.338
495.484	489.348	-1.238	187.597	0.107	14.433	22.173	14.341	22.298
519.998	511.653	-1.605	198.255	0.108	14.845	22.693	14.723	22.860
589.538	584.075	-0.927	225.466	0.108	15.852	24.128	15.776	24.230
653.219	646.290	-1.061	251.436	0.108	16.758	25.340	16.667	25.464
706.613	706.767	0.022	272.514	0.108	17.460	26.423	17.462	26.420

TABLE IX

Calculated Data for DS123; Load Factor = (P_s/P_{amb})

u_{meas}	u_{derivd}	% diff	Re	rho	x	y	x_{der}	y_{der}
152.104	140.978	-7.314	25.852	0.048	3.673	5.345	3.563	5.507
205.643	191.446	-6.904	34.826	0.048	4.138	6.021	4.021	6.193
255.344	234.030	-8.347	43.371	0.048	4.517	6.524	4.363	6.753
297.951	279.856	-6.073	50.695	0.048	4.808	7.007	4.689	7.182
356.476	343.239	-3.713	61.022	0.048	5.178	7.614	5.101	7.728
403.269	389.851	-3.327	69.122	0.048	5.443	8.011	5.370	8.119
458.958	447.222	-2.557	78.903	0.049	5.739	8.468	5.680	8.556
501.628	467.058	-6.892	86.306	0.049	5.949	8.618	5.781	8.865
544.924	523.058	-4.013	94.300	0.049	6.163	9.034	6.063	9.182
597.093	566.723	-5.086	103.407	0.049	6.395	9.328	6.263	9.523
704.387	644.581	-8.491	123.114	0.049	6.857	9.852	6.618	10.205
777.374	677.579	-12.837	137.120	0.049	7.159	10.086	6.776	10.651
134.822	141.747	5.137	36.672	0.077	4.224	6.446	4.310	6.320
206.685	218.855	5.888	56.336	0.077	5.016	7.659	5.132	7.488
256.233	264.[illegible]39	3.109	69.681	0.077	5.461	8.244	5.528	8.145
296.868	301.151	1.443	80.839	0.077	5.79[illegible]	8.687	5.828	8.638
344.020	346.108	0.607	94.199	0.078	6.161	9.200	6.175	9.178
386.201	383.527	-0.692	106.322	0.078	6.466	9.602	6.448	9.629
448.419	441.481	-1.547	123.774	0.078	6.872	10.164	6.829	10.227
494.887	481.346	-2.736	136.810	0.078	7.152	10.525	7.073	10.641
549.970	535.635	-2.607	153.029	0.078	7.480	11.009	7.402	11.125
609.705	590.650	-3.125	168.621	0.078	7.776	11.417	7.678	11.562
680.228	641.696	-5.665	189.977	0.078	8.156	11.845	7.968	12.122
184.926	218.083	17.930	68.930	0.106	5.437	8.657	5.808	8.110
216.346	248.706	14.957	81.168	0.106	5.804	9.143	6.137	8.652
244.572	274.239	12.130	91.967	0.107	6.102	9.513	6.388	9.091
288.444	316.163	9.610	108.337	0.106	6.515	10.060	6.758	9.701
344.023	370.116	7.585	129.603	0.107	6.999	10.722	7.207	10.415
380.224	404.794	6.462	143.761	0.107	7.296	11.125	7.481	10.852
448.291	469.308	4.688	170.062	0.107	7.803	11.814	7.947	11.601
495.484	509.031	2.734	187.597	0.107	8.115	12.191	8.203	12.062
519.998	529.684	1.863	198.255	0.108	8.296	12.420	8.358	12.329
589.538	598.415	1.506	225.466	0.108	8.734	13.053	8.787	12.976
653.219	651.474	-0.267	251.436	0.108	9.124	13.536	9.114	13.550
706.613	698.713	-1.118	272.514	0.108	9.422	13.928	9.380	13.991

TABLE I

Calculated Data for DS123; Load Factor = $(P_s/P_{amb} * T_f/T_a)$

u_{meas}	u_{derivd}	% diff	Re	rho	x	y	x_{der}	y_{der}
152.104	134.627	-11.490	25.852	0.048	3.794	5.467	3.609	5.706
205.643	189.620	-7.791	34.826	0.048	4.287	6.161	4.147	6.341
255.344	236.721	-7.293	43.371	0.048	4.691	6.677	4.547	6.862
297.951	288.006	-3.338	50.695	0.048	5.001	7.173	4.932	7.262
356.476	359.411	0.823	61.022	0.048	5.396	7.795	5.414	7.771
403.269	412.524	2.295	69.122	0.048	5.679	8.205	5.732	8.136
458.958	478.248	4.203	78.903	0.049	5.995	8.676	6.097	8.544
501.628	501.274	-0.071	86.306	0.049	6.220	8.832	6.218	8.834
544.924	565.717	3.816	94.300	0.049	6.450	9.259	6.550	9.131
597.093	616.770	3.295	103.407	0.049	6.698	9.567	6.788	9.451
704.387	708.886	0.639	123.114	0.049	7.195	10.116	7.214	10.092
777.374	749.052	-3.643	137.120	0.049	7.520	10.364	7.406	10.511
134.822	130.307	-3.349	36.672	0.077	4.379	6.382	4.318	6.460
206.685	209.484	1.354	56.336	0.077	5.222	7.584	5.251	7.547
256.233	256.729	0.193	69.681	0.077	5.697	8.166	5.702	8.160
296.868	295.406	-0.492	80.839	0.077	6.055	8.606	6.043	8.622
344.020	342.711	-0.380	94.199	0.078	6.447	9.114	6.437	9.127
386.201	382.224	-1.030	106.322	0.078	6.775	9.513	6.746	9.550
448.419	443.886	-1.011	123.774	0.078	7.211	10.073	7.181	10.112
494.887	486.632	-1.668	136.810	0.078	7.513	10.435	7.461	10.502
549.970	544.849	-0.931	153.029	0.078	7.866	10.919	7.836	10.957
609.705	605.113	-0.753	168.621	0.078	8.185	11.336	8.160	11.369
680.228	660.886	-2.844	189.977	0.078	8.595	11.768	8.494	11.898
184.926	201.541	8.985	68.930	0.106	5.672	8.390	5.876	8.128
216.346	231.842	7.163	81.168	0.106	6.065	8.860	6.240	8.635
244.572	257.292	5.201	91.967	0.107	6.384	9.219	6.518	9.046
288.444	299.291	3.761	108.337	0.106	6.827	9.752	6.932	9.618
344.023	353.574	2.776	129.603	0.107	7.348	10.396	7.431	10.289
380.224	388.543	2.188	143.761	0.107	7.667	10.789	7.735	10.701
448.291	453.855	1.241	170.062	0.107	8.214	11.460	8.256	11.406
495.484	494.795	-0.139	187.597	0.107	8.551	11.835	8.546	11.841
519.998	515.673	-0.832	198.255	0.108	8.747	12.055	8.717	12.094
589.538	586.317	-0.546	225.466	0.108	9.221	12.678	9.200	12.705
653.219	641.162	-1.846	251.436	0.108	9.642	13.154	9.569	13.248
706.613	690.843	-2.232	272.514	0.108	9.966	13.547	9.874	13.666

TABLE XI

Calculated Data for DS14567; Full Velocity and Temperature Range

u_{meas}	u_{derivd}	% diff	Re	rho	x	y	x_{der}	y_{der}
152.104	146.605	-3.615	25.852	0.048	3.794	4.776	3.737	4.841
205.643	202.671	-1.445	34.826	0.048	4.287	5.377	4.262	5.407
255.344	249.926	-2.122	43.372	0.048	4.691	5.823	4.650	5.870
297.951	300.588	0.885	50.696	0.048	5.001	6.246	5.019	6.226
356.476	370.659	3.979	61.024	0.048	5.396	6.779	5.483	6.679
403.269	421.699	4.570	69.124	0.048	5.679	7.124	5.784	7.004
458.958	484.142	5.487	78.906	0.049	5.995	7.519	6.128	7.367
501.628	505.066	0.685	86.310	0.049	6.220	7.645	6.237	7.625
544.924	565.480	3.772	94.306	0.049	6.450	8.002	6.549	7.889
597.093	611.316	2.382	103.415	0.049	6.699	8.248	6.763	8.174
704.387	689.216	-2.154	123.127	0.049	7.195	8.670	7.131	8.744
777.374	718.257	-7.605	137.138	0.049	7.520	8.841	7.280	9.117
354.361	367.268	3.642	58.189	0.047	5.292	6.649	5.370	6.559
404.538	422.015	4.320	66.644	0.047	5.594	7.019	5.692	6.907
449.815	461.815	2.668	74.463	0.048	5.855	7.278	5.918	7.205
501.415	504.033	0.522	82.993	0.047	6.121	7.526	6.134	7.511
563.094	561.678	-0.252	93.667	0.048	6.432	7.860	6.425	7.868
616.618	605.252	-1.843	102.949	0.048	6.686	8.101	6.635	8.160
706.261	667.155	-5.537	118.949	0.048	7.094	8.440	6.930	8.628
788.933	696.168	-11.758	133.934	0.048	7.448	8.606	7.075	9.034
197.723	199.096	0.694	32.265	0.047	4.155	5.269	4.167	5.255
257.739	271.233	5.236	42.140	0.047	4.636	5.919	4.734	5.807
309.777	334.434	7.960	50.742	0.047	5.003	6.411	5.162	6.228
348.912	383.289	9.853	57.233	0.047	5.256	6.755	5.462	6.518
396.795	438.422	10.491	65.334	0.047	5.549	7.120	5.781	6.855
194.506	178.415	-8.273	30.500	0.046	4.060	4.984	3.919	5.146
250.818	239.492	-4.516	39.415	0.046	4.510	5.566	4.426	5.663
297.159	301.230	1.370	46.813	0.046	4.840	6.072	4.867	6.041
353.618	373.817	5.712	55.804	0.046	5.202	6.593	5.321	6.456
394.105	425.049	7.852	62.426	0.046	5.446	6.934	5.618	6.737
452.096	489.048	8.173	71.644	0.046	5.763	7.316	5.951	7.100
491.215	526.563	7.196	78.282	0.046	5.976	7.543	6.149	7.345
556.689	569.811	2.357	88.906	0.046	6.296	7.781	6.356	7.712
596.104	595.570	-0.090	95.452	0.047	6.482	7.923	6.480	7.925
696.213	660.463	-5.135	112.602	0.047	6.936	8.277	6.788	8.447
135.998	98.210	-27.786	24.297	0.050	3.699	4.201	3.237	4.732
195.498	170.944	-12.560	35.032	0.050	4.298	5.155	4.068	5.419
248.365	238.065	-4.147	44.539	0.050	4.742	5.835	4.661	5.929
309.721	315.189	1.766	55.689	0.050	5.197	6.494	5.235	6.451
353.610	366.342	3.601	63.717	0.050	5.492	6.882	5.572	6.789
395.026	412.875	4.519	71.289	0.050	5.751	7.207	5.856	7.086
453.760	478.547	5.463	82.277	0.050	6.099	7.640	6.234	7.486
502.164	525.564	4.660	91.136	0.050	6.360	7.923	6.480	7.786
556.507	574.707	3.270	101.492	0.050	6.647	8.216	6.735	8.115

TABLE XI (Cont'd)

Calculated Data for DS14567; Full Velocity and Temperature Range

u_{meas}	u_{derivd}	% diff	Re	rho	x	y	x_{der}	y_{der}
599.269	604.303	0.840	109.822	0.050	6.866	8.393	6.889	8.366
702.823	683.538	-2.744	129.902	0.051	7.355	8.831	7.272	8.927
209.757	195.040	-7.016	31.422	0.045	4.110	5.065	3.989	5.204
261.510	253.576	-3.034	39.180	0.045	4.499	5.585	4.443	5.650
302.723	288.079	-4.838	45.487	0.045	4.783	5.866	4.687	5.976
350.912	340.657	-2.922	52.822	0.045	5.086	6.252	5.024	6.323
408.037	409.935	0.465	61.520	0.045	5.414	6.711	5.424	6.699
459.691	474.229	3.163	69.605	0.045	5.695	7.106	5.768	7.022
500.760	508.631	1.572	76.011	0.045	5.904	7.306	5.942	7.262
559.019	564.082	0.906	85.124	0.045	6.185	7.610	6.208	7.584
596.469	588.122	-1.399	91.104	0.045	6.359	7.743	6.323	7.785
702.287	622.198	-11.404	108.195	0.045	6.824	7.938	6.493	8.318

TABLE XII

Calculated Data for DS14567mod; Limited Velocity Range

u_{meas}	u_{derivd}	% diff	Re	rho	x	y	x_{der}	y_{der}
255.344	243.345	-4.699	43.372	0.048	4.517	5.757	4.431	5.860
297.951	293.741	-1.413	50.696	0.048	4.808	6.175	4.781	6.208
356.476	363.767	2.045	61.024	0.048	5.178	6.700	5.221	6.650
403.269	414.896	2.883	69.124	0.048	5.443	7.041	5.505	6.967
458.958	477.611	4.064	78.906	0.049	5.739	7.430	5.831	7.320
501.628	498.598	-0.604	86.310	0.049	5.949	7.554	5.934	7.571
544.924	559.488	2.673	94.306	0.049	6.163	7.905	6.229	7.827
597.093	605.620	1.428	103.415	0.049	6.395	8.148	6.431	8.104
704.387	683.911	-2.907	123.127	0.049	6.857	8.560	6.777	8.657
354.361	361.330	1.967	58.189	0.047	5.081	6.581	5.121	6.533
404.538	416.357	2.922	66.644	0.047	5.364	6.946	5.426	6.872
449.815	456.421	1.468	74.463	0.048	5.608	7.202	5.640	7.163
501.415	498.924	-0.497	82.993	0.047	5.856	7.446	5.845	7.460
563.094	557.049	-1.074	93.667	0.048	6.147	7.776	6.120	7.807
616.618	601.005	-2.532	102.949	0.048	6.383	8.012	6.318	8.090
706.261	663.459	-6.060	118.949	0.048	6.763	8.345	6.596	8.544
250.818	234.193	-6.628	39.415	0.046	4.348	5.517	4.230	5.657
297.159	295.928	-0.414	46.813	0.046	4.657	6.018	4.650	6.027
353.618	368.839	4.304	55.804	0.046	4.997	6.534	5.081	6.433
394.105	420.486	6.694	62.426	0.046	5.226	6.871	5.363	6.707
452.096	485.089	7.298	71.644	0.046	5.522	7.249	5.679	7.060
491.215	523.062	6.483	78.282	0.046	5.721	7.472	5.866	7.298
556.689	566.728	1.803	88.906	0.046	6.020	7.707	6.063	7.656
596.104	592.807	-0.553	95.452	0.047	6.193	7.847	6.179	7.863
696.213	658.346	-5.439	112.602	0.047	6.616	8.194	6.470	8.369
248.365	230.624	-7.143	44.539	0.050	4.566	5.758	4.432	5.918
309.721	307.092	-0.849	55.689	0.050	4.992	6.407	4.975	6.428
353.610	358.011	1.245	63.717	0.050	5.269	6.789	5.295	6.758
395.026	404.437	2.382	71.289	0.050	5.511	7.110	5.563	7.047
453.760	470.119	3.605	82.277	0.050	5.836	7.536	5.919	7.436
502.164	517.182	2.991	91.136	0.050	6.080	7.813	6.152	7.727
556.507	566.411	1.780	101.492	0.050	6.347	8.101	6.392	8.047
599.269	596.021	-0.542	109.822	0.050	6.551	8.273	6.536	8.290
702.823	675.257	-3.922	129.902	0.051	7.006	8.701	6.894	8.834
261.510	248.939	-4.807	39.180	0.045	4.337	5.544	4.253	5.645
302.723	283.522	-6.343	45.487	0.045	4.604	5.821	4.485	5.964
350.912	336.389	-4.139	52.822	0.045	4.888	6.205	4.806	6.303
408.037	406.277	-0.431	61.520	0.045	5.195	6.659	5.186	6.670
459.691	471.353	2.537	69.605	0.045	5.458	7.050	5.513	6.985
500.760	506.232	1.093	76.011	0.045	5.654	7.248	5.679	7.218
559.019	562.466	0.617	85.124	0.045	5.916	7.549	5.930	7.532
596.469	586.848	-1.613	91.104	0.045	6.079	7.679	6.039	7.726

TABLE XIII

Calculated Data for DS146; Limited Temperature Range

u_{meas}	u_{derivd}	% diff	Re	rho	x	y	x_{der}	y_{der}
152.104	149.018	-2.029	25.852	0.048	3.225	4.866	3.201	4.905
205.643	202.937	-1.315	34.826	0.048	3.590	5.480	3.573	5.508
255.344	248.702	-2.601	43.371	0.048	3.885	5.934	3.848	5.995
297.951	298.172	0.074	50.695	0.048	4.109	6.367	4.111	6.365
356.476	367.216	3.013	61.022	0.048	4.393	6.911	4.440	6.833
403.269	418.026	3.659	69.122	0.048	4.595	7.265	4.655	7.166
458.958	480.733	4.744	78.903	0.049	4.819	7.670	4.900	7.536
501.628	501.981	0.070	86.306	0.049	4.977	7.799	4.978	7.797
544.924	563.413	3.393	94.300	0.049	5.138	8.166	5.200	8.063
597.093	610.507	2.247	103.407	0.049	5.312	8.420	5.354	8.350
704.387	691.964	-1.764	123.114	0.049	5.656	8.858	5.620	8.918
777.374	723.437	-6.938	137.120	0.049	5.880	9.039	5.729	9.287
354.361	361.839	2.110	58.188	0.047	4.319	6.764	4.351	6.710
404.538	415.840	2.794	66.642	0.047	4.535	7.142	4.580	7.067
449.815	455.470	1.257	74.460	0.048	4.719	7.407	4.741	7.372
501.415	497.770	-0.727	82.989	0.047	4.907	7.661	4.894	7.682
563.094	556.068	-1.248	93.661	0.048	5.126	8.004	5.103	8.043
616.618	600.549	-2.606	102.941	0.048	5.303	8.252	5.253	8.335
706.261	664.501	-5.913	118.937	0.048	5.586	8.602	5.465	8.802
788.933	695.549	-11.837	133.917	0.048	5.830	8.778	5.571	9.205
197.723	198.697	0.493	32.265	0.047	3.493	5.357	3.499	5.347
257.739	268.131	4.032	42.139	0.047	3.845	6.020	3.900	5.929
309.777	329.613	6.403	50.741	0.047	4.111	6.521	4.204	6.368
348.912	377.522	8.200	57.231	0.047	4.293	6.872	4.416	6.668
396.795	432.043	8.883	65.332	0.047	4.502	7.245	4.642	7.014
135.998	103.120	-24.175	24.297	0.050	3.154	4.294	2.855	4.788
195.498	173.380	-11.314	35.031	0.050	3.598	5.269	3.445	5.520
248.365	238.829	-3.840	44.539	0.050	3.922	5.966	3.867	6.057
309.721	314.909	1.675	55.688	0.050	4.251	6.641	4.276	6.599
353.610	365.931	3.485	63.715	0.050	4.462	7.038	4.517	6.947
395.026	412.729	4.482	71.286	0.050	4.646	7.373	4.720	7.251
453.760	479.413	5.653	82.273	0.050	4.892	7.818	4.990	7.657
502.164	527.618	5.069	91.131	0.050	5.076	8.110	5.167	7.960
556.507	578.546	3.960	101.485	0.050	5.276	8.413	5.350	8.291
599.269	609.605	1.725	109.813	0.050	5.428	8.597	5.461	8.541
702.823	693.553	-1.319	129.888	0.051	5.766	9.054	5.739	9.099

TABLE XIV

Calculated Data for DS145; Limited Temperature Range

u_{meas}	u_{derivd}	% diff	Re	rho	x	y	x_{der}	y_{der}
152.104	136.236	-10.432	25.852	0.048	3.794	4.776	3.627	4.960
205.643	192.643	-6.321	34.826	0.048	4.287	5.377	4.174	5.502
255.344	240.753	-5.714	43.372	0.048	4.691	5.823	4.579	5.946
297.951	292.679	-1.769	50.696	0.048	5.001	6.246	4.964	6.286
356.476	365.039	2.402	61.024	0.048	5.396	6.779	5.449	6.721
403.269	417.965	3.644	69.124	0.048	5.679	7.124	5.763	7.032
458.958	482.996	5.237	78.906	0.049	5.995	7.519	6.122	7.380
501.628	504.835	0.639	86.310	0.049	6.220	7.645	6.236	7.627
544.924	568.111	4.255	94.306	0.049	6.450	8.002	6.561	7.880
597.093	616.152	3.192	103.415	0.049	6.699	8.248	6.785	8.153
704.387	698.210	-0.877	123.127	0.049	7.195	8.670	7.169	8.699
777.374	729.022	-6.220	137.138	0.049	7.520	8.841	7.325	9.056
354.361	360.765	1.807	58.189	0.047	5.292	6.649	5.331	6.606
404.538	417.497	3.203	66.644	0.047	5.594	7.019	5.667	6.939
449.815	458.935	2.027	74.463	0.048	5.855	7.278	5.903	7.225
501.415	502.891	0.295	82.993	0.047	6.121	7.526	6.128	7.518
563.094	563.187	0.016	93.667	0.048	6.432	7.860	6.432	7.860
616.618	608.879	-1.255	102.949	0.048	6.686	8.101	6.652	8.139
706.261	674.032	-4.563	118.949	0.048	7.094	8.440	6.960	8.588
788.933	704.733	-10.673	133.934	0.048	7.448	8.606	7.111	8.977
197.723	188.554	-4.637	32.265	0.047	4.155	5.269	4.075	5.357
257.739	261.956	1.636	42.140	0.047	4.636	5.919	4.667	5.885
309.777	326.856	5.513	50.742	0.047	5.003	6.411	5.114	6.288
348.912	377.302	8.137	57.233	0.047	5.256	6.755	5.427	6.567
396.795	434.513	9.506	65.334	0.047	5.549	7.120	5.759	6.889
194.506	167.219	-14.029	30.500	0.046	4.060	4.984	3.816	5.252
250.818	228.999	-8.699	39.415	0.046	4.510	5.566	4.345	5.747
297.159	292.072	-1.712	46.813	0.046	4.840	6.072	4.806	6.110
353.618	366.778	3.721	55.804	0.046	5.202	6.593	5.280	6.507
394.105	419.841	6.530	62.426	0.046	5.446	6.934	5.589	6.776
452.096	486.305	7.567	71.644	0.046	5.763	7.316	5.938	7.124
491.215	525.507	6.981	78.282	0.046	5.976	7.543	6.143	7.358
556.689	570.696	2.516	88.906	0.046	6.296	7.781	6.360	7.710
596.104	597.690	0.266	95.452	0.047	6.482	7.923	6.489	7.915
696.213	665.927	-4.350	112.602	0.047	6.936	8.277	6.811	8.414

TABLE XV

Calculated Data for DS146mod; Limited Velocity and Temperature Range

u_{meas}	u_{derivd}	% diff	Re	rho	x	y	x_{der}	y_{der}
255.344	241.216	-5.533	43.372	0.048	4.350	5.757	4.255	5.877
297.951	291.868	-2.041	50.696	0.048	4.623	6.175	4.586	6.222
356.476	362.531	1.693	61.024	0.048	4.970	6.700	5.003	6.659
403.269	414.279	2.730	69.124	0.048	5.217	7.041	5.273	6.971
458.958	477.932	4.134	78.906	0.049	5.494	7.430	5.581	7.320
501.628	499.271	-0.470	86.310	0.049	5.689	7.554	5.679	7.567
544.924	561.311	3.007	94.306	0.049	5.889	7.905	5.958	7.819
597.093	608.378	1.890	103.415	0.049	6.105	8.148	6.150	8.091
704.387	688.511	-2.254	123.127	0.049	6.535	8.560	6.477	8.633
354.361	359.859	1.552	58.189	0.047	4.879	6.581	4.908	6.544
404.538	415.518	2.714	66.644	0.047	5.144	6.946	5.198	6.878
449.815	456.152	1.409	74.463	0.048	5.371	7.202	5.400	7.165
501.415	499.303	-0.421	82.993	0.047	5.603	7.446	5.594	7.458
563.094	558.474	-0.821	93.667	0.048	5.874	7.776	5.855	7.799
616.618	603.308	-2.158	102.949	0.048	6.094	8.012	6.043	8.078
706.261	667.171	-5.535	118.949	0.048	6.447	8.345	6.306	8.523
248.365	228.607	-7.955	44.539	0.050	4.396	5.758	4.256	5.935
309.721	305.539	-1.350	55.689	0.050	4.796	6.407	4.770	6.439
353.610	356.973	0.951	63.717	0.050	5.054	6.789	5.073	6.766
395.026	403.990	2.269	71.289	0.050	5.281	7.110	5.327	7.051
453.760	470.707	3.735	82.277	0.050	5.584	7.536	5.665	7.434
502.164	518.610	3.275	91.136	0.050	5.811	7.813	5.885	7.721
556.507	568.849	2.218	101.492	0.050	6.060	8.101	6.113	8.035
599.269	599.131	-0.023	109.822	0.050	6.250	8.273	6.249	8.274
702.823	680.291	-3.206	129.902	0.051	6.673	8.701	6.589	8.807

TABLE XVI

Calculated Data for DS145mod; Limited Velocity and Temperature Range

u_{meas}	u_{derivd}	% diff	Re	rho	x	y	x_{der}	y_{der}
255.344	238.340	-6.659	43.372	0.048	4.517	5.823	4.394	5.968
297.951	289.571	-2.812	50.696	0.048	4.808	6.246	4.754	6.311
356.476	361.100	1.297	61.024	0.048	5.178	6.779	5.205	6.747
403.269	413.514	2.540	69.124	0.048	5.443	7.124	5.498	7.059
458.958	478.018	4.153	78.906	0.049	5.739	7.519	5.833	7.408
501.628	499.705	-0.383	86.310	0.049	5.949	7.645	5.940	7.655
544.924	562.614	3.246	94.306	0.049	6.163	8.002	6.243	7.908
597.093	610.430	2.234	103.415	0.049	6.395	8.248	6.452	8.181
704.387	692.252	-1.723	123.127	0.049	6.857	8.670	6.810	8.726
354.361	356.870	0.708	58.189	0.047	5.081	6.649	5.095	6.632
404.538	413.025	2.098	66.644	0.047	5.364	7.019	5.409	6.966
449.815	454.099	0.952	74.463	0.048	5.608	7.278	5.629	7.253
501.415	497.713	-0.738	82.993	0.047	5.856	7.526	5.839	7.546
563.094	557.622	-0.972	93.667	0.048	6.147	7.860	6.123	7.889
616.618	603.080	-2.195	102.949	0.048	6.383	8.101	6.327	8.168
706.261	667.995	-5.418	118.949	0.048	6.763	8.440	6.614	8.616
250.818	226.846	-9.557	39.415	0.046	4.348	5.566	4.177	5.768
297.159	289.025	-2.737	46.813	0.046	4.657	6.072	4.606	6.133
353.618	362.820	2.602	55.804	0.046	4.997	6.593	5.048	6.533
394.105	415.328	5.385	62.426	0.046	5.226	6.934	5.337	6.803
452.096	481.197	6.437	71.644	0.046	5.522	7.316	5.661	7.152
491.215	520.104	5.881	78.282	0.046	5.721	7.543	5.853	7.387
556.689	564.996	1.492	88.906	0.046	6.020	7.781	6.055	7.739
596.104	591.837	-0.716	95.452	0.047	6.193	7.923	6.175	7.944
696.213	659.775	-5.234	112.602	0.047	6.616	8.277	6.476	8.443

TABLE XVII

Calculated Data for DS1457mod; Limited Velocity and Temperature Range

u_{meas}	u_{derivd}	% diff	Re	rho	x	y	x_{der}	y_{der}
255.344	242.821	-4.905	43.372	0.048	4.517	5.757	4.427	5.864
297.951	293.339	-1.548	50.696	0.048	4.808	6.175	4.778	6.211
356.476	363.574	1.991	61.024	0.048	5.178	6.700	5.219	6.652
403.269	414.872	2.877	69.124	0.048	5.443	7.041	5.505	6.967
458.958	477.814	4.108	78.906	0.049	5.739	7.430	5.832	7.319
501.628	498.881	-0.547	86.310	0.049	5.949	7.554	5.936	7.569
544.924	560.019	2.770	94.306	0.049	6.163	7.905	6.231	7.825
597.093	606.341	1.549	103.415	0.049	6.395	8.148	6.434	8.101
704.387	684.983	-2.755	123.127	0.049	6.857	8.560	6.781	8.651
354.361	361.075	1.895	58.189	0.047	5.081	6.581	5.119	6.535
404.538	416.280	2.903	66.644	0.047	5.364	6.946	5.426	6.873
449.815	456.489	1.484	74.463	0.048	5.608	7.202	5.641	7.163
501.415	499.145	-0.453	82.993	0.047	5.856	7.446	5.846	7.459
563.094	557.501	-0.993	93.667	0.048	6.147	7.776	6.122	7.805
616.618	601.640	-2.429	102.949	0.048	6.383	8.012	6.321	8.087
706.261	664.371	-5.931	118.949	0.048	6.763	8.345	6.600	8.539
250.818	233.568	-6.877	39.415	0.046	4.348	5.517	4.226	5.662
297.159	295.439	-0.579	46.813	0.046	4.657	6.018	4.647	6.031
353.618	368.551	4.223	55.804	0.046	4.997	6.534	5.080	6.435
394.105	420.365	6.663	62.426	0.046	5.226	6.871	5.362	6.708
452.096	485.190	7.320	71.644	0.046	5.522	7.249	5.680	7.060
491.215	523.311	6.534	78.282	0.046	5.721	7.472	5.868	7.298
556.689	567.146	1.878	88.906	0.046	6.020	7.707	6.065	7.654
596.104	593.333	-0.465	95.452	0.047	6.193	7.847	6.182	7.860
696.213	659.159	-5.322	112.602	0.047	6.616	8.194	6.473	8.364
261.510	248.290	-5.055	39.180	0.045	4.337	5.544	4.248	5.650
302.723	282.948	-6.533	45.487	0.045	4.604	5.821	4.481	5.968
350.912	335.946	-4.265	52.822	0.045	4.888	6.205	4.803	6.306
408.037	406.037	-0.490	61.520	0.045	5.195	6.659	5.185	6.672
459.691	471.331	2.532	69.605	0.045	5.458	7.050	5.513	6.985
500.760	506.336	1.113	76.011	0.045	5.654	7.248	5.679	7.218
559.019	562.783	0.673	85.124	0.045	5.916	7.549	5.932	7.530
596.469	587.264	-1.543	91.104	0.045	6.079	7.679	6.041	7.724

TABLE XVIII

Sensor 2 Data for DS14567; X_n = .38, X_0 = -.5

u_{meas}	u_{derivd}	% diff	Re	rho	x	y	x_{der}	y_{der}
152.104	151.117	-0.649	25.852	0.048	3.442	4.292	3.433	4.302
205.643	205.822	0.087	34.826	0.048	3.854	4.808	3.855	4.806
255.344	250.841	-1.764	43.372	0.048	4.189	5.181	4.161	5.215
297.951	299.159	0.405	50.697	0.048	4.445	5.536	4.452	5.528
356.476	368.120	3.266	61.026	0.048	4.770	5.995	4.828	5.924
403.269	422.368	4.736	69.128	0.048	5.001	6.315	5.090	6.206
458.958	485.823	5.853	78.912	0.049	5.259	6.662	5.374	6.521
501.628	497.748	-0.774	86.317	0.049	5.441	6.724	5.425	6.744
544.924	561.647	3.069	94.315	0.049	5.628	7.051	5.693	6.971
597.093	612.527	2.585	103.427	0.049	5.829	7.286	5.885	7.216
704.387	695.188	-1.306	123.146	0.049	6.228	7.666	6.197	7.704
777.374	711.494	-8.475	137.164	0.049	6.489	7.760	6.274	8.022
354.361	371.731	4.902	58.192	0.047	4.684	5.924	4.770	5.820
404.538	424.306	4.887	66.648	0.047	4.932	6.232	5.022	6.122
449.815	468.645	4.186	74.467	0.048	5.145	6.480	5.225	6.381
501.415	514.275	2.565	83.000	0.047	5.361	6.709	5.413	6.646
563.094	570.908	1.388	93.676	0.048	5.613	6.990	5.643	6.954
616.618	610.980	-0.914	102.961	0.048	5.819	7.179	5.798	7.204
706.261	677.281	-4.103	118.967	0.048	6.147	7.487	6.050	7.605
788.933	734.335	-6.920	133.960	0.048	6.431	7.740	6.258	7.951
197.723	211.291	6.862	32.265	0.047	3.744	4.788	3.839	4.671
257.739	283.211	9.883	42.141	0.047	4.144	5.344	4.295	5.159
309.777	344.681	11.267	50.744	0.047	4.447	5.754	4.631	5.530
348.912	392.992	12.634	57.235	0.047	4.655	6.046	4.870	5.784
396.795	449.750	13.346	65.337	0.047	4.895	6.368	5.134	6.077
194.506	173.659	-10.718	30.501	0.046	3.665	4.386	3.510	4.575
250.818	240.274	-4.204	39.416	0.046	4.040	4.953	3.974	5.033
297.159	303.498	2.133	46.814	0.046	4.313	5.408	4.347	5.366
353.618	375.875	6.294	55.806	0.046	4.610	5.861	4.719	5.729
394.105	423.426	7.440	62.429	0.046	4.811	6.137	4.944	5.974
452.096	484.561	7.181	71.648	0.046	5.070	6.455	5.205	6.290
491.215	526.752	7.234	78.288	0.046	5.243	6.674	5.384	6.502
556.689	573.035	2.936	88.914	0.046	5.503	6.893	5.564	6.819
596.104	599.821	0.624	95.462	0.047	5.654	7.019	5.667	7.003
696.213	653.986	-6.065	112.619	0.047	6.020	7.278	5.879	7.450
135.998	99.753	-26.651	24.297	0.050	3.361	3.748	2.988	4.204
195.498	170.986	-12.538	35.032	0.050	3.863	4.582	3.671	4.817
248.365	235.605	-5.138	44.540	0.050	4.232	5.165	4.148	5.267
309.721	310.221	0.161	55.691	0.050	4.607	5.728	4.610	5.725
353.610	364.370	3.043	63.720	0.050	4.849	6.088	4.904	6.020
395.026	411.495	4.169	71.292	0.050	5.060	6.375	5.139	6.278
453.760	474.422	4.553	82.283	0.050	5.343	6.735	5.435	6.624
502.164	526.210	4.789	91.144	0.050	5.555	7.004	5.655	6.883
556.507	584.289	4.992	101.502	0.050	5.787	7.298	5.895	7.166
599.269	622.602	3.894	109.834	0.050	5.963	7.487	6.050	7.381

TABLE XVIII (Cont'd)

Sensor 2 Data for DS14567; X_n = .38, X_o = -.5

u_{meas}	u_{derivd}	% diff	Re	rho	x	y	x_{der}	y_{der}
702.823	669.161	-4.789	129.923	0.051	6.356	7.717	6.239	7.861
209.757	183.325	-12.601	31.422	0.045	3.706	4.400	3.521	4.626
261.510	241.322	-7.720	39.180	0.045	4.031	4.873	3.909	5.021
302.723	284.175	-6.127	45.488	0.045	4.266	5.185	4.165	5.309
350.912	340.097	-3.082	52.824	0.045	4.515	5.548	4.462	5.613
408.037	410.584	0.624	61.523	0.045	4.784	5.956	4.796	5.942
459.691	472.216	2.725	69.609	0.045	5.014	6.285	5.066	6.222
500.760	497.451	-0.661	76.017	0.045	5.185	6.415	5.172	6.431
559.019	544.358	-2.623	85.131	0.045	5.413	6.643	5.359	6.709
596.469	560.758	-5.987	91.114	0.045	5.554	6.725	5.426	6.882
702.287	569.505	-18.907	108.210	0.046	5.930	6.786	5.476	7.340

TABLE XII

Sensor 2 Data for DS14567mod; X_n = .37, Y_0 = -.56

u_{meas}	u_{derivd}	% diff	Re	rho	x	y	x_{der}	y_{der}
255.344	245.025	-4.041	43.372	0.048	4.034	5.064	3.973	5.141
297.951	292.912	-1.691	50.697	0.048	4.274	5.410	4.247	5.444
356.476	361.511	1.412	61.026	0.048	4.578	5.858	4.601	5.828
403.269	415.546	3.044	69.128	0.048	4.794	6.168	4.847	6.101
458.958	478.840	4.332	78.912	0.049	5.034	6.505	5.114	6.405
501.628	490.570	-2.204	86.317	0.049	5.204	6.565	5.161	6.619
544.924	554.431	1.745	94.315	0.049	5.378	6.882	5.412	6.838
597.093	605.108	1.342	103.427	0.049	5.564	7.109	5.592	7.074
704.387	686.823	-2.494	123.146	0.049	5.935	7.473	5.880	7.543
354.361	367.498	3.707	58.192	0.047	4.498	5.804	4.559	5.727
404.538	420.256	3.888	66.648	0.047	4.729	6.104	4.797	6.019
449.815	464.768	3.324	74.467	0.048	4.928	6.345	4.987	6.270
501.415	510.537	1.819	83.000	0.047	5.129	6.568	5.164	6.524
563.094	567.263	0.740	93.676	0.048	5.364	6.840	5.379	6.821
616.618	607.290	-1.513	102.961	0.048	5.555	7.023	5.524	7.062
706.261	673.449	-4.646	118.967	0.048	5.860	7.318	5.758	7.448
250.818	237.469	-5.322	39.416	0.046	3.894	4.866	3.816	4.964
297.159	300.986	1.288	46.814	0.046	4.150	5.312	4.170	5.287
353.618	373.949	5.749	55.806	0.046	4.429	5.756	4.521	5.639
394.105	421.987	7.075	62.429	0.046	4.616	6.026	4.735	5.876
452.096	483.731	6.997	71.648	0.046	4.858	6.337	4.981	6.181
491.215	526.422	7.167	78.288	0.046	5.020	6.550	5.150	6.386
556.689	572.986	2.927	88.914	0.046	5.262	6.763	5.318	6.692
596.104	600.009	0.655	95.462	0.047	5.402	6.885	5.415	6.869
696.213	653.976	-6.067	112.619	0.047	5.742	7.133	5.611	7.299
248.365	227.727	-8.309	44.540	0.050	4.074	5.029	3.945	5.192
309.721	301.048	-2.800	55.691	0.050	4.425	5.577	4.379	5.635
353.610	354.405	0.225	63.720	0.050	4.651	5.926	4.655	5.921
395.026	400.892	1.485	71.292	0.050	4.849	6.204	4.875	6.170
453.760	463.008	2.038	82.283	0.050	5.113	6.552	5.151	6.504
502.164	514.133	2.384	91.144	0.050	5.310	6.812	5.357	6.753
556.507	571.419	2.680	101.502	0.050	5.526	7.094	5.580	7.025
599.269	609.084	1.638	109.834	0.050	5.689	7.275	5.724	7.232
702.823	653.849	-6.968	129.923	0.051	6.054	7.491	5.895	7.693
261.510	240.130	-8.176	39.180	0.045	3.885	4.801	3.765	4.953
302.723	283.419	-6.377	45.488	0.045	4.106	5.107	4.007	5.232
350.912	340.076	-3.088	52.824	0.045	4.340	5.464	4.290	5.527
408.037	411.655	0.887	61.523	0.045	4.591	5.864	4.606	5.845
459.691	474.349	3.189	69.609	0.045	4.806	6.187	4.862	6.116
500.760	499.985	-0.155	76.017	0.045	4.965	6.314	4.962	6.317
559.019	547.566	-2.049	85.131	0.045	5.178	6.536	5.138	6.586
596.469	564.090	-5.428	91.114	0.045	5.309	6.615	5.201	6.752

TABLE XX

Sensor 2 Data for DS146mod; X_n = .37, X_o = -.54

u_{meas}	u_{derivd}	% diff	Re	rho	x	y	x_{der}	y_{der}
255.344	243.189	-4.760	43.372	0.048	4.034	5.103	3.962	5.194
297.951	291.269	-2.243	50.697	0.048	4.274	5.452	4.238	5.497
356.476	360.250	1.059	61.026	0.048	4.578	5.903	4.595	5.881
403.269	414.665	2.826	69.128	0.048	4.794	6.217	4.843	6.154
458.958	478.493	4.256	78.912	0.049	5.034	6.557	5.113	6.458
501.628	490.392	-2.240	86.317	0.049	5.204	6.618	5.161	6.673
544.924	554.898	1.830	94.315	0.049	5.378	6.938	5.414	6.892
597.093	606.183	1.522	103.427	0.049	5.564	7.167	5.596	7.128
704.387	689.267	-2.147	123.146	0.049	5.935	7.537	5.888	7.597
354.361	365.251	3.073	58.192	0.047	4.498	5.844	4.548	5.780
404.538	418.245	3.388	66.648	0.047	4.729	6.147	4.788	6.072
449.815	463.018	2.935	74.467	0.048	4.928	6.390	4.981	6.323
501.415	509.099	1.533	83.000	0.047	5.129	6.615	5.158	6.578
563.094	566.346	0.577	93.676	0.048	5.364	6.889	5.376	6.875
616.618	606.825	-1.588	102.961	0.048	5.555	7.075	5.522	7.116
706.261	673.854	-4.589	118.967	0.048	5.860	7.374	5.759	7.502
248.365	226.773	-8.694	44.540	0.050	4.074	5.074	3.939	5.244
309.721	300.638	-2.932	55.691	0.050	4.425	5.627	4.377	5.688
353.610	354.491	0.249	63.720	0.050	4.651	5.979	4.656	5.974
395.026	401.476	1.633	71.292	0.050	4.849	6.260	4.878	6.223
453.760	464.365	2.337	82.283	0.050	5.113	6.613	5.157	6.557
502.164	516.185	2.792	91.144	0.050	5.310	6.875	5.364	6.806
556.507	574.369	3.210	101.502	0.050	5.526	7.161	5.591	7.079
599.269	612.723	2.245	109.834	0.050	5.689	7.345	5.736	7.286
702.823	658.717	-6.275	129.923	0.051	6.054	7.566	5.911	7.747

Appendix C

Test Equipment

Table XXI provides a list of all equipment used during this experiment.

TABLE XXI

Test Equipment

ITEM	MAKE	MODEL	S/N	USE
1.	Endevco Power Supply	4225	AC12	Provide power to all but ambient pressure transducers
2.	Endevco Signal Conditioner	4423	AE82	Amplify signal of pressure transducer PT#0
			AF02	Amplify signal of pressure transducer PT#1
			AE80	Amplify signal of pressure transducer PT#2
3.	Bell & Howell Pressure Transducers	CEC1000-02	8986	PT#0 (0-50 psivg) measures static pressure, P_s
			7726	PT#1 (0-100 psivg) measures source pressure, P_{source}
			9294	PT#2 (0-50 psivg) measures calibrator total pressure, P_o
4.	TSI Platinum Hot Film Sensor	1241-10	J875	Sensor to measure velocity changes
5.	TSI Intelligent Flow Analyzer	150	144D(Ch3)	Measured resistance and voltage changes due to velocity for Ch1 of sensor
			336F(Ch5)	Measured resistance and voltage changes due to velocity for Ch2 of sensor
6.	Tektronix Oscilloscope	465M	B022081	Display sensor frequency response
7.	Tektronix Polaroid Camera	C-30 Ser	B016460	Photograph frequency response signal off of oscilloscope
8.	Hewlett-Packard 3052A Data Acquisition System	HP9845B	183A03293	Computer/Thermal Printer
		HP9885M	1628A12413	Master Flexible Drive
			1629A05355	Slave Flexible Drive
		HP3455A	1622A09432	Digital Voltmeter
		HP3495A	1428A06961	Scanner

TABLE XII (Cont'd)

Test Equipment

ITEM	MAKE	MODEL	S/N	USE
		HP3437A		System Voltmeter
		HP9871A		Impact Printer
		HP9872S		Plotter
9.	HP Dual DC Power Supply	HP6205C	2208A-00632	Power for ambient pressure transducer
10.	CEC DC Bridge Balance	8-108	26003	
11.	MKS Air Calibrator Portable Vacuum Standard		44362-1	Calibrate CEC pressure transducers and pressure gages
12.	Hot Wire Calibrator with VARIAC autotransformer	NONE	NONE	Calibrate hot-wire or hot-films
13.	Pressure Gages			
	Heise (0-30 psi)	NONE	H43234	measured static pressure, P_s
	Wallace & Tiernan (0-100 psi)	FA145	PP13097	measured total pressure, P_o
	Wallace & Tiernan (0-30 in Hg)	FA145	HH10973	$P_o - P_s$

Bibliography

1. Bradshaw, Peter. An Introduction to Turbulence and Its Measurement. New York: Pergamon Press, 1971.

2. Bulletin TB5. Hot Film & Hot Wire Anemometry, Theory and Application. Thermo-Systems, Inc.; St. Paul, Minnesota, 1982.

3. Collis, D. C. and Williams, M. J. "Two-dimensional Convection from Heated Wires at Low Reynolds Numbers," Journal of Fluid Mechanics, Vol 6: 357-384 (Oct 1959).

4. Dougherty, John J. The Calibration and Use of a Hot-Wire Anemometer With the Hewlett-Packard 3054A Data Acquisition System. AFWAL-TR-85-2008, July 1985.

5. Freymouth, P. A Bibliography of Thermal Anemometry, Thermo-Systems, Inc.; St. Paul, Minnesota, 1982.

6. Holman, J. P. Experimental Methods for Engineers (Third Ed.) New York: McGraw-Hill Book Company, 1978.

7. John, J. E. A. Gas Dynamics. Boston: Allyn and Bacon, Inc., 1977.

8. Kays, W. M. and Crawford, M. E. Convective Heat and Mass Transfer (Second Ed.). New York: McGraw-Hill Book Company, 1980.

9. Keenan, J. H. and others. Gas Tables (Second Ed.). New York: John Wiley and Sons, Inc., 1980.

10. McQueen, Capt. Steve M. Velocity and Transient Measurements in a Shock Tube Using a Hot-Wire Anemometer, MS Thesis, GAE/AA/84D-17. School of Engineering, Air Force Institute of Technology (AU), WPAFB, Ohio, December 1984.

11. Norman, Bo. Hot Wire Anemometer Calibration at High Subsonic Speeds. DISA Information No. 5, Denmark: DISA Electronik Pub., Jun 1967.

12. Rivir, Richard B. Personal Communication. AFWAL Aero Propulsion Laboratory, WPAFB, Ohio, October 1986 to January 1987.

13. Thermo-Systems, Inc. Hot Wire/Hot Film Anemometry Probes and Accessories, St. Paul, Minnesota, 1983.

14. Vonada, J. Personal Notes. Air Force Institute of Technology, WPAFB, Ohio, March 1982.

Vita

Captain Denise C. Oka was born on 11 February 1957 in Cincinnati, Ohio. She graduated from Seton High School in 1975 and attended the University of Cincinnati from which she received the degree of Bachelor of Science in Aerospace Engineering in June 1980. Upon graduation, she received a commission in the US Air Force through the ROTC training program and entered active duty in October 1980. Her first assignment was to the Aero Propulsion Laboratory's Ramjet Engine Division where she managed ramjet missile development programs and conducted an inhouse inlet test. In January 1984 she took on the job of Executive Officer for the Laboratory and in November of 1984 became a deputy program manager for the T-46A Simulator Program in ASD's Simulator SPO until entering into the Master of Science program in Aeronautical Engineering at the Air Force Institute of Technology at Wright Patterson AFB, Ohio.

Permanent Address: 1393 Devils Backbone Road
Cincinnati, Ohio 45233

UNCLASSIFIED

SECURITY CLASSIFICATION OF THIS PAGE

ADA189717

REPORT DOCUMENTATION PAGE

Form Approved OMB No 0704-0188

1a REPORT SECURITY CLASSIFICATION: Unclassified	1b RESTRICTIVE MARKINGS
2a. SECURITY CLASSIFICATION AUTHORITY	3 DISTRIBUTION/AVAILABILITY OF REPORT: Approved for public release; distribution unlimited.
2b DECLASSIFICATION/DOWNGRADING SCHEDULE	
4 PERFORMING ORGANIZATION REPORT NUMBER(S): AFIT/GAE/AA/86D-12	5 MONITORING ORGANIZATION REPORT NUMBER(S)
6a. NAME OF PERFORMING ORGANIZATION: AFIT School of Engineering; 6b. OFFICE SYMBOL (If applicable): AFIT/ENY	7a. NAME OF MONITORING ORGANIZATION
6c. ADDRESS (City, State, and ZIP Code): Air Force Institute of Technology, Wright-Patterson AFB, Oh 45433	7b ADDRESS (City, State, and ZIP Code)
8a. NAME OF FUNDING/SPONSORING ORGANIZATION; 8b. OFFICE SYMBOL (If applicable)	9 PROCUREMENT INSTRUMENT IDENTIFICATION NUMBER
8c. ADDRESS (City, State, and ZIP Code)	10. SOURCE OF FUNDING NUMBERS: PROGRAM ELEMENT NO; PROJECT NO; TASK NO; WORK UNIT ACCESSION NO.

11. TITLE (Include Security Classification)
Calibration of a Hot-Wire/Hot-Film Anemometer Over a Range of Temperatures, Velocities, and Pressures (Unclassified)

12. PERSONAL AUTHOR(S)
Denise C Oka, Capt, USAF

13a. TYPE OF REPORT	13b TIME COVERED	14. DATE OF REPORT (Year, Month, Day)	15. PAGE COUNT
MS Thesis	FROM ____ TO ____	1987 September	95

16. SUPPLEMENTARY NOTATION

17. COSATI CODES		
FIELD	GROUP	SUB-GROUP
14	02	Instrumentation

18. SUBJECT TERMS (Continue on reverse if necessary and identify by block number)
Hot-wire, hot-film, calibration, wide range of temperatures, pressures and velocities, single calibration equation.

19. ABSTRACT (Continue on reverse if necessary and identify by block number)

Thesis Advisor: Dr. William C. Elrod

Lynn Wolan 29 Oct 87

Abstract (Unclassified)

The possibility of developing a single calibration equation that would be applicable to a wide range of temperatures (68F to 250F), velocities (150 to 800 ft/sec), and pressures (15 to 33 psia) was investigated. A platinum hot-film, with high operating temperature to provide adequate sensitivity to velocity, was calibrated at seven different temperature/pressure conditions. The calibration data was used to calculate velocity, Reynolds number and Nusselt number and a linear least squares curve fit applied to Reynolds number raised to an exponent and Nusselt number times a load factor raised to an exponent. The exponents were chosen, through an iterative process, to provide the best agreement between the data and the curve fit equation. The results indicate that as the range of conditions is allowed to increase, so does the error between measured velocity and velocity

20. DISTRIBUTION/AVAILABILITY OF ABSTRACT: ☐ UNCLASSIFIED/UNLIMITED ☒ SAME AS RPT ☐ DTIC USERS	21 ABSTRACT SECURITY CLASSIFICATION: Unclassified
22a NAME OF RESPONSIBLE INDIVIDUAL: Dr. William C. Elrod	22b TELEPHONE (Include Area Code): 513-255-3517; 22c OFFICE SYMBOL: AFIT/ENY

DD Form 1473, JUN 86 — Previous editions are obsolete — SECURITY CLASSIFICATION OF THIS PAGE

Unclassified

Block 19 (cont)

derived from the calibration equation. The least deviation in the velocities occured for curve fits of individual data sets giving an average of 0.8% to 2.5% difference. When several different temperature or several different pressure curves were collapsed to a single curve, the error could be minimized to 2.5% to 3.1% if the velocity range was limited to 300 to 700 ft/sec.

END